MASARYKOVA UNIVERZITA
PŘÍRODOVĚDECKÁ FAKULTA
ÚSTAV TEORETICKÉ FYZIKY A ASTROFYZIKY

Bakalářská práce

SAMUEL FABO

MASARYKOVA UNIVERZITA

PŘÍRODOVĚDECKÁ FAKULTA
ÚSTAV TEORETICKÉ FYZIKY A ASTROFYZIKY

Excetrické zákrytové dvojhězdy

Bakalářská práce

Samuel Fabo

Vedoucí práce: doc. RNDr. Miloslav Zejda, Ph.D.
Brno 2024

Bibliografický záznam

Autor: Samuel Fabo
Přírodovědecká fakulta, Masarykova univerzita
Ústav teoretické fyziky a astrofyziky

Název práce: Excetrické zákrytové dvojhězdy

Studijní program: Fyzika

Studijní obor: Astrofyzika

Vedoucí práce: doc. RNDr. Miloslav Zejda, Ph.D.

Akademický rok: 2023/24

Počet stran: VI + 46

Klíčová slova: Proměnné hvězdy; Zákrytové dvojhvězdy; Fotometrie; Světelná křivka; $O-C$ diagram; TESS; ASAS-SN

Bibliographic Entry

Author: Samuel Fabo
                       Faculty of Science, Masaryk University
                       Department of Theoretical Physics and Astrophysics

Title of Thesis: Eccentric eclipsing binaries

Degree Programme: Physics

Field of Study: Astrophysics

Supervisor: doc. RNDr. Miloslav Zejda, Ph.D.

Academic Year: 2023/24

Number of Pages: VI $+$ 46

Keywords: Variable stars; Eclipsing binaries; Photometry; Light curve;
                       $O - C$ diagram; TESS; ASAS-SN

Abstrakt

Tato bakalářská práce se zabývá studiem 21 objektů, identifikovaných jako zákrytové dvojhvězdy s excetrickými drahami, které dosud nebyly dostatečně prozkoumány. Hlavním cílem bylo zpracování fotometrických dat z družice TESS a přehlídky ASAS-SN a určení časů minim světelných křivek. Z těchto časů, doplněných o další dostupná data, byly vytvořeny O-C diagramy, které byly následně analyzovány. Snažili jsme se dokázat nebo případně vyvrátit excentricitu systémů a také v nich najít některé zajímavé jevy. V článku jsou také shrnuty základní informace o objektech, které již byly známy nebo získány pomocí zpracovaných dat. Pokusili sme se o zpřesnění základních efemerid.

Abstract

The bachelor thesis focuses on the study of 21 objects identified as eclipsing binaries with eccentric orbits, which have not yet been sufficiently studied. The main objective was the processing of photometric data from the TESS satellite and the ASAS-SN survey and the determination of the minima timings of the light curves. From these times, complemented by other available data, O-C diagrams were constructed and subsequently analysed. We attempted to prove or possibly disprove the excetricity of the systems and also to find some interesting phenomena in them. Also, basic information about the objects that were already known or obtained using the processed data is summarized in the thesis. An attempt has been made to specify the basic ephemeris.

MUNI
SCI

ZADÁNÍ
BAKALÁŘSKÉ PRÁCE

Akademický rok: 2023/2024

Ústav:	Ústav teoretické fyziky a astrofyziky
Student:	Samuel Fabo
Program:	Fyzika
Specializace:	Astrofyzika

Ředitel *ústavu* PřF MU Vám ve smyslu Studijního a zkušebního řádu MU určuje bakalářskou práci s názvem:

Název práce:	Excentrické zákrytové dvojhvězdy
Název práce anglicky:	Eccentric eclipsing binaries
Jazyk závěrečné práce:	angličtina

Oficiální zadání:
Zákrytové dvojhvězdy s eliptickými trajektoriemi představují specifickou skupinu dvojhvězd. Lze jich využít k například určení interní struktury jejich složek, ověření OTR, verifikaci našich představ o struktuře hvězdných soustav i jejich vývoji. Znalost přesných orbitálních parametrů těchto systémů je proto klíčová. Student se bude zabývat hvězdami, u kterých je podezření na excentrickou dráhu, avšak pro většinu z nich dosud nebyl proveden řádný výzkum. Z archivu družice TESS zpracuje fotometrická data pro vybraný soubor dvojhvězd, potvrdí, případně vyvrátí nenulovou excentricitu a určí okamžiky minim světelných křivek. Z těchto časů s využitím dalších dostupných dat sestaví O-C diagramy pro tyto dvojhvězdné soustavy a provede jejich analýzu.

Literatura:
BUDDING, E. a Osman DEMIRCAN. *A guide to close binary systems*. Online. First edition. Boca Raton: CRC Press, 2022. viii, 352. ISBN 9781032226866. [citováno 2024-04-23]

Vedoucí práce:	doc. RNDr. Miloslav Zejda, Ph.D.
Konzultant:	Mgr. Jakub Kolář
Datum zadání práce:	11. 10. 2023
V Brně dne:	23. 4. 2024

Zadání bylo schváleno prostřednictvím IS MU.

Samuel Fabo, 12. 11. 2023
doc. RNDr. Miloslav Zejda, Ph.D., 11. 10. 2023
RNDr. Luboš Poláček, 5. 12. 2023

Poděkování

Na tomto místě bych chtěl poděkovat svému vedoucímu práce doc. RNDr. Miloslavu Zejdovi, Ph.D. a konzultantovi Mgr. Jakubovi Kolářovi za cenné rady, vstřícný přístup a čas, který mi věnovali při konzultacích a počas celého psaní této práce.

Prohlášení

Prohlašuji, že jsem svoji bakalářskou práci vypracoval samostatně pod vedením vedoucího práce a konzultanta s využitím informačních zdrojů, které jsou v práci citovány.

Brno 12. května 2024

. . . .
Samuel Fabo

Contents

Introduction

Astrophysics has been greatly advanced by the study of variable stars, which began about half a millennium ago. This includes a subgroup of geometric variables that change their brightness due to external factors, such as eclipsing binaries. These systems consist of two stars orbiting around the common center of gravity, and as seen from Earth, they are mutually occulting. Thanks to this phenomenon, we can directly measure brightness decrease. Eclipsing binaries with eccentric orbits are particularly interesting because their orbits are not circular but elliptical. Analysis of this variability allows us to study the dynamic properties of these systems, test models of stellar evolution, etc.

The main goal of this bachelor thesis was a study of 21 eclipsing binaries with eccentric orbits, that are not widely published or properly studied. To achieve this goal, we processed photometric data from the TESS satellite and the ASAS-SN survey, and then we constructed the light curves, and determined the minima timings from this data. Subsequently, these minimum times were compared with the calculated values based on existing ephemeris which allowed us to compile O-C diagrams. The analysis of these diagrams revealed, in some cases, deviations from the predicted behavior and made it possible to detect certain phenomena in the studied objects. In addition to diagrams, this thesis also focused on summarizing basic information about all 21 objects, such as their phase, magnitudes, and periods.

In the first part, we discuss a brief history of variable stars and the basic concepts in the field. The second part discusses the methods used to obtain the data, the sources from which they were taken for this thesis, and describes the post-processing of these data. All data used were obtained by photometry, which measures the intensity of light coming from a source. A recent breakthrough in this field is the TESS satellite, which has very precise measurements, and also the ASAS-SN project, which continuously covers the entire night sky with 24 telescopes. The main part of the thesis is the fourth chapter, where we summarise and describe the results of the practical part.

Chapter 1

Variable stars

1.1 What are variable stars?

Almost all stars change their brightness. Sometimes, these changes are subtle, but sometimes, they can be very significant. It depends on the star itself and especially on the process behind the changes. These changes over time can range from a few milliseconds to decades. In some cases, it can be millions or billions of years. At the same time, the changes in brightness are in the range of several orders of magnitude. However, not all stars that change their brightness are defined as variable stars. Even the Sun changes its brightness with a period of about 11 years, but these changes are not significant. One possibility of a variable star that we can see with our own eyes are novae or supernovae. These have the most pronounced changes. However, they are very rare and disappear after a short time. But the universe is dominated by stars that change brightness almost all their lives. Variable stars are then divided into several categories based on different criteria. The two basic groups are extrinsic and intrinsic variables. This division is mainly conditioned by the cause of the variability of the stars (see chapter 1.3).

The study of variable stars is very important in astrophysics because it allows us to obtain necessary information. After processing the observed data by various methods, such as photometry and subsequent construction of so-called light curves, we can determine, for example, the distance of the system, the absolute magnitude, the period, etc. This allows us to study their internal structure and evolutionary stages and then it can be applied to other stars, clusters, or even galaxy structures. Nowadays, we get data from various space sources (TESS, KEPLER, Hipparcos, Gaia, . . .) and ground-based surveys (ASAS, OGLE, 2MASS, . . .). Astrophysics started to advance a lot with the advent of telescopes and automated surveys, as they started to produce large amounts of data, whereas, in the past, each star had to be studied individually for a long time. At the same time, we acquire data by various methods such as spectroscopy, photometry, etc. We can further process this data by different methods to make them more relevant.

1.2 History

Variable stars have a rich history that spans centuries of astronomical observation and discovery. From the earliest known records of variable stars in ancient China, Egypt, and

Greece to the cutting-edge research of modern astronomy, the study of variable stars has played a key role in our understanding of the universe.

One of the earliest recorded observations of a variable star comes from China, where astronomers noted the changing brightness of the star Algol in the constellation Perseus. However, recent studies show that brightness changes of this star were observed about 3 000 years earlier in Egypt (Jetsu et al., 2013). Another important milestone for astronomy, which took place in Greece, was when the astronomer Hipparchus compiled the first catalog of stars that included several variable stars too (Percy, 2007).

An advance in astronomy especially in the field of variable stars came in 1572 when Tycho Brahe observed a supernova and from the collected data he plotted the dependence of brightness on time and as the first who call it a light curve. However, nothing of it was systematic observations of variable stars until the 18th century. In those times were first systematic observations made by astronomers such as John Goodricke and Edward Pigott. Goodricke was particularly interested in the star Algol, which he observed to vary in brightness over a period of 2.87 days. He was the first to propose that the variability of Algol and other similar stars was due to their external factors, such as eclipses. Other astronomers later confirmed this idea, and the study of variable stars became an important area of research in astronomy. Over time, many different types of variable stars were identified and classified based on their light curves and other characteristics.

One of the first studied groups was the pulsating stars in the 19th century, especially the Cepheids. Later, there were discovered some other types of variable stars including RR Lyrae stars, which are similar to Cepheids but have shorter periods and lower luminosities or cataclysmic variables, which are binary star systems that undergo sudden and dramatic increases in brightness due to accretion events. The study of variable stars has also led to the discovery of exotic objects, such as pulsars and black holes, which exhibit variability in their emission of radiation.

In addition to their scientific importance, variable stars have also played a role in cultural and artistic traditions throughout history. For example, the star Algol has been associated with various mythological and astrological beliefs and has been referenced in literature and art for centuries.

Today, variable stars continue to be an important area of research in astronomy, providing insights into the evolution and behavior of stars and serving as important tools for measuring distances in the universe. The study of variable stars is also closely tied to other areas of astronomy, such as the search for exoplanets and the study of stellar populations in galaxies. Overall, the history of variable stars is a testament to the power of observation and discovery in astronomy, and to the ongoing quest to understand the nature of the universe.

1.3 Types of variable stars

1.3.1 Extrinsic variable stars

There are several reasons why the brightness of objects may change. One of the causes is the geometry of the system itself. Stars that change their brightness in this way are called extrinsic variables. There are no changes within the star itself, the luminosity does not change. All that variations is the amount of signal (photon count) that we observe.

Rotation variables

Rapid rotation exerts influence on a star's shape and luminosity. Centrifugal force causes the star to bulge at the equator, resulting in an ellipsoid. This deformation leads to a larger emitting area at the equator than at the poles which causes periodic changes in the star's brightness since the intensity of the emission is proportional to the area. A similar phenomenon is observed in close binary stars where the gravitational interaction between the stars distorts their shapes thus forming tidal bulges. These bulges lead to brightness variability due to the changing orientations of the tidal bulge.

The next possible reason for the brightness change are spots on the star's surface. These can be of two types. The spots may have a different temperature than the rest of the star's surface and thus warmer and cooler parts of stars appear and disappear in our direction. But also the spots on the star's surface can have a different chemical composition. These stars are called chemically peculiar.

Variations can also occur in close binaries, where there is a shape deformation due to gravity or the "spilling" of mass from one component to another.

Eclipsing binaries

The components of such a binary star orbit around a common center of gravity and at the same time regularly eclipse from our point of view. As this topic is the main focus of the thesis, it is discussed in more detail in the section 1.4.

1.3.2 Intrinsic variable stars

Unlike extrinsic variables, in this case, changes of star luminosities are driven by processes in stellar interiors. Intrinsic variable stars are subdivided into eruptive and pulsating stars.

Pulsating stars

Some types of stars exhibit a phenomenon known as pulsation, which means that they periodically change size and temperature, leading to fluctuations in their luminosity. Studying the pulsations allows us to probe the internal structure and composition of these stars and some of them are an essential tool in determining galactic distances. Typical representatives are Cepheids, RR Lyrae, Delta Scuti, and Mira variables.

Cepheids were studied by Henrietta Swan Leavitt in the late 19th century and she noticed an interesting characteristic of them. She found a correlation between the period of a Cepheid's variability and its absolute brightness and she combined it all into one relation.

$$M_V = -2.81 \log(P) - 1.43, \tag{1.1}$$

where M_V is a absolute magnitude and P is period of star (in days) (Mikulášek and Zejda, 2013). This discovery allowed astronomers to use Cepheids as "standard candles" for measuring distances in the universe. Thus, they played a key role in the development of our understanding of the size and structure of the universe.

Eruptive stars

Some stars suddenly change their brightness. This can be due to the interaction of binary stars or various catastrophic processes. They are known as erupting stars. Novae, supernovae, hypernovae, symbiotic variables, cataclysmic variables, and some young stars belong to this class.

1.4   Eclipsing binaries

As already mentioned, an eclipsing binary (hereafter EB) is a pair of stars that orbit around a common center of gravity. The orbital plane must lie edge-on to us so that the components can periodically eclipse each other. This will only occur if the angle of inclination i reaches a value close to $90°$ (Zeilik and Gregory, 1998).
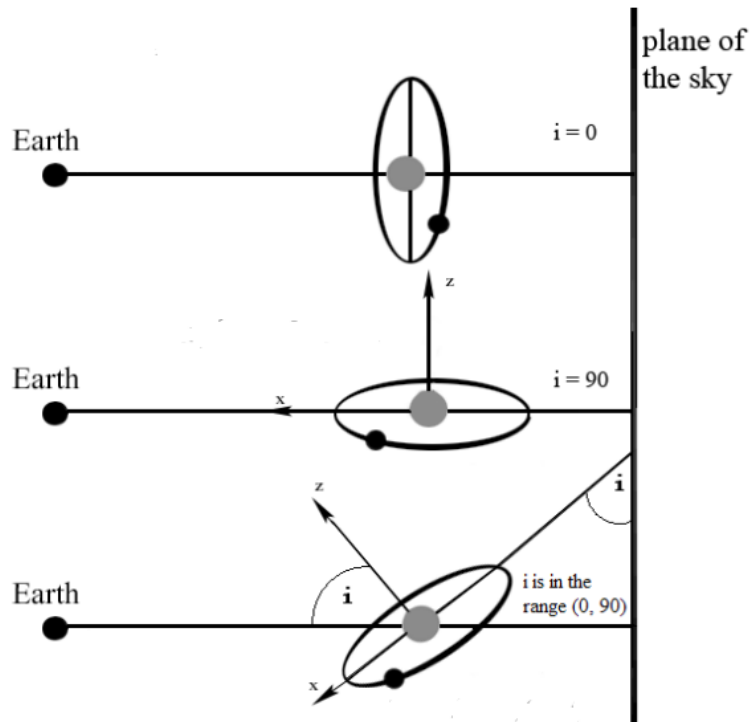
Figure 1.1: Illustration of inclination.

More precisely, the condition must be fulfilled: $i > 90° - \alpha$,

$$\sin \alpha = \frac{R_1 + R_2}{r}, \tag{1.2}$$

where R_1, R_2 are radii of the components and r is their distance (Mikulášek and Zejda, 2013).

   If an eclipse already happens, it can be total or partial. It depends on the inclination and the size of both components. If a minor component passes in the foreground, this is

called a transit (this can also be used, for example, in the search for and exploration of exoplanets). Otherwise, it is an occultation. We can recognize whether it is a transition or an occultation from the light curves.
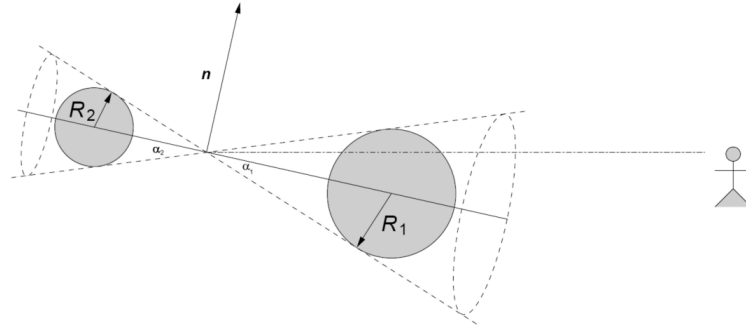
Figure 1.2: Occultation scheme shows under what conditions eclipses happen in the direction to the observer. (Mikulášek and Zejda, 2013) (Created by Jiří Krtička).

1.4.1 Light curves

Light curves are graphs of luminosity or more precisely change in luminosity as a function of time. For data processing and description of periodic variable stars, it is convenient to use the so-called *phase function* ϑ. It is the sum of two functions: the *epoch E* and the *phase* φ

$$\vartheta(t) = E(t) + \varphi(t), \tag{1.3}$$

where

$$E(t) = \text{floor}(\vartheta(t)); \quad \varphi(t) = \text{frac}(\vartheta(t)). \tag{1.4}$$

The function *floor* always rounds down to an integer part of the ϑ value. So it is a non-decreasing function that increases by 1 after each period P. In the opposite, the *frac* function is periodic and takes only decimal part values. Using the *phase* we can construct a so-called *phase curve*. We calculate it using the ϑ

$$\varphi = \text{frac}(\vartheta) = \text{frac}\frac{t - M_0}{P}, \tag{1.5}$$

where t is the actual time of observation and M_0 is an initial moment. Phase takes values from 0 to 1. Unlike the whole light curve, it shows us only changes during one cycle of the system, i.e. in one period. It serves us to recognize the type of variable stars. Whether they are pulsating stars or EBs as in our case. EBs are further subdivided according to light curves into: EA type or Algol (β Persei), EB known as β Lyrae type, and EW or W UMa type (Čokina et al., 2021).

Algol type

This subgroup is characterized, in particular, by the fact that the brightness is not changing between the eclipses (see figure 1.3). Compared to the constant brightness outside the

eclipses, they have a very significant primary minimum during the eclipsing. This primary minimum is caused by eclipse of small hot component by larger and cooler star, thus tends to be narrow and deep. The opposite situation, when a hot star transits in front of a cooler component, causes a shallow secondary minimum. In some parts of spectra, the minimum is even unobservable.

In most cases, both the beginning and the end of the minimum are clearly discernible on the light curves. As for the range of brightness changes, it can go from hundredths mag to several mag. The amplitudes of the changes sometimes vary with respect to the filters in which we observe. The large range also applies to the orbital period. Algol types have a large range of periods from a few minutes to even several days (Sterken and Jaschek, 1996).
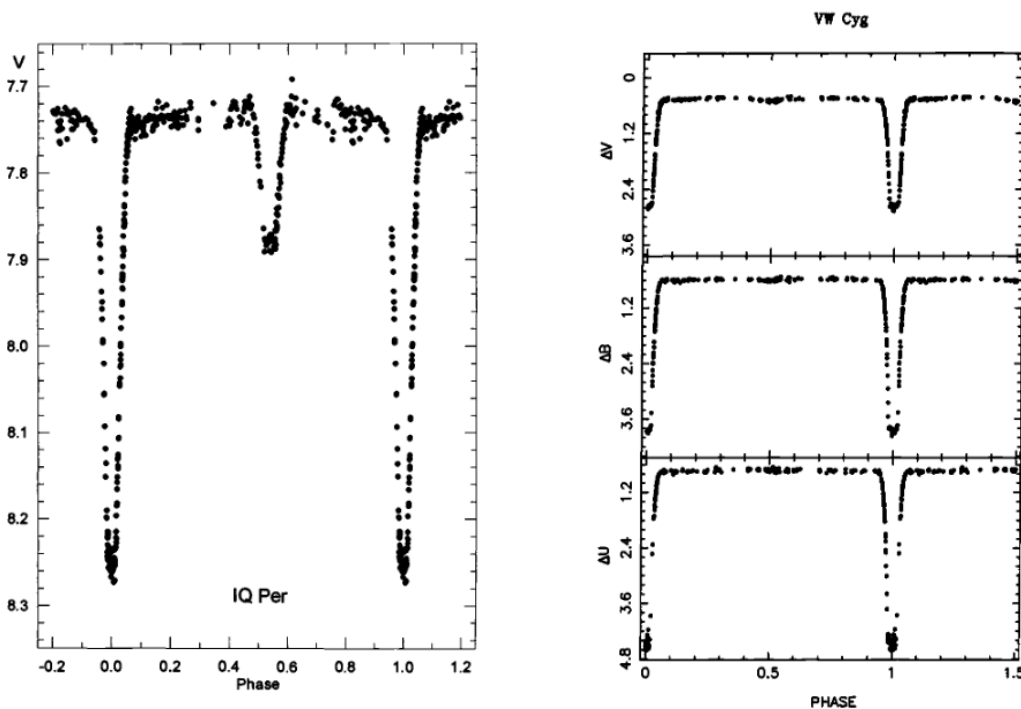
Figure 1.3: Example of phase curve of Algol type binary and difference in the depth of minimum in *UBV* filters (Sterken and Jaschek, 1996).

β Lyrae type

At first sight, this type has a different shape of light curve than the previous one as can be seen in figure 1.4. The luminosity varies gradually between eclipses. This makes it almost impossible to determine the exact beginning and end of the eclipse. This shape of the curve clearly indicates the presence of tidal forces between the components. Their shapes are quite ellipsoidal and probably at least one component fills the Roche lobe. The periods are usually longer than 0.5 d, but can reach hundreds of days for giant stars. The luminosity varies by less than 2 mag (Sterken and Jaschek, 1996).
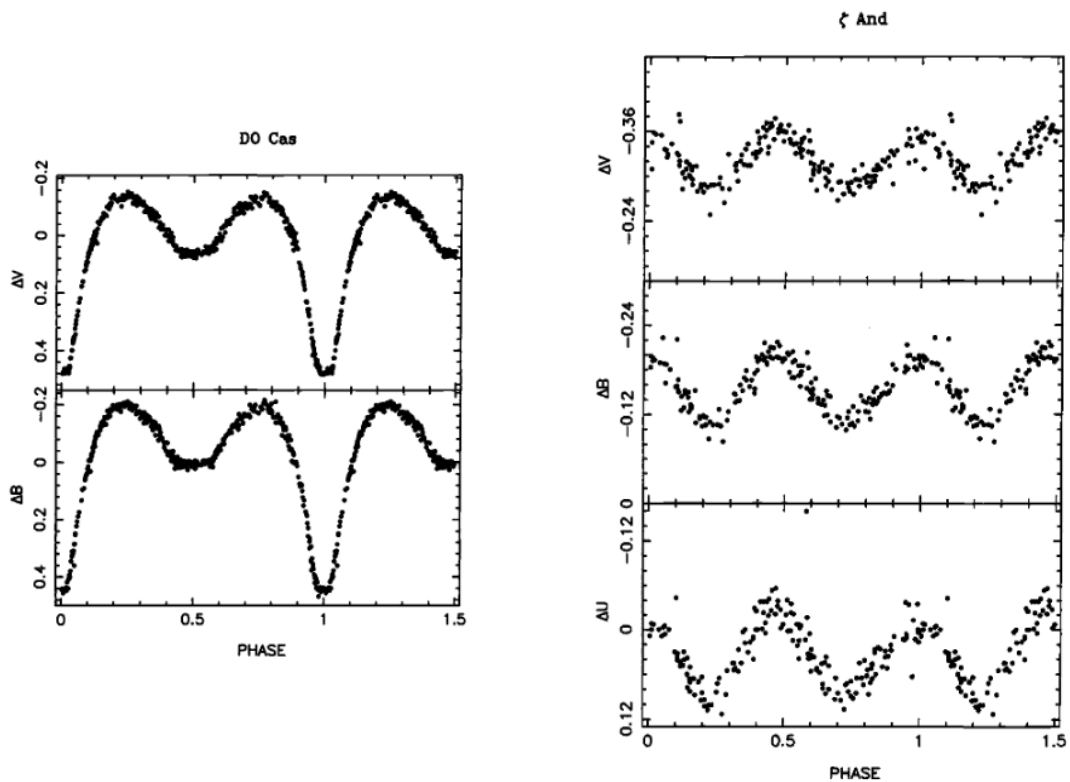
Figure 1.4: Example of phase curve of β Lyrea type binary and difference in phase curve in different filters. (Sterken and Jaschek, 1996).

W UMa type

Components of W UMa type systems fill their Roche lobes, leading to an ellipsoidal shape. They are usually in contact or almost in contact with similar temperature.

The light curve looks similar to that β Lyrae type, i.e., the light changes decreases and increases gradually between eclipses. It is impossible to determine the exact beginning and end of the changes. The main difference is that the W UMa types have nearly equal deep primary and secondary minima and variability changes range from a few tenths to less than a magnitude. There is also a difference in periods, where one orbit takes less than a day in this case. W UMa type stars are further subdivided into two groups according to the different characteristics of the systems, namely W- and A-type (Sterken and Jaschek, 1996).
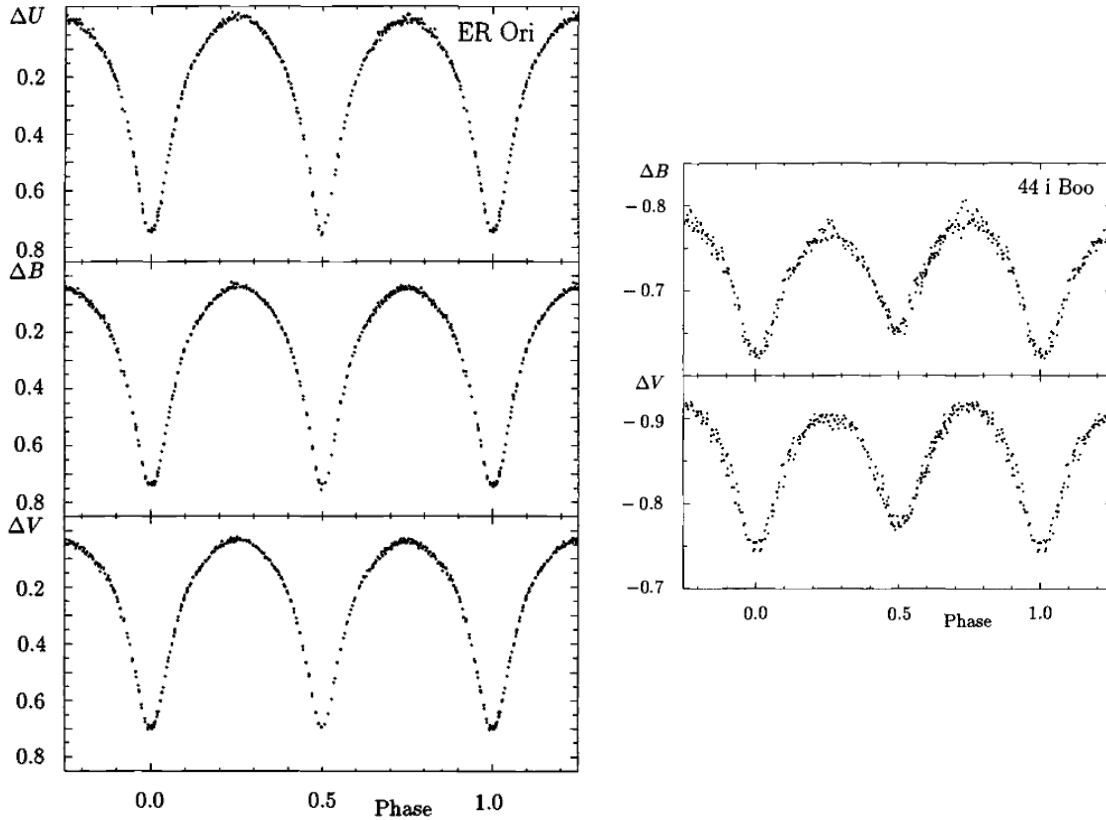
Figure 1.5: Example phase curves of W UMa type binaries (Sterken and Jaschek, 1996).

1.4.2 Why do we observe EBs?

Binaries, and especially EBs, offer us much more information than stars that do not change their brightness. H. N. Russell described EBs as the "royal road" to stellar astrophysics. Photometric observations, the measurement of their changing brightness, provide crucial data for studying these systems. While advancements have facilitated data acquisition through space-based and ground-based surveys, citizen science initiatives utilizing readily available equipment have also contributed significantly. However, the accuracy and detail of data obtained by amateur astronomers are often not comparable to those collected by professional observatories.

By photometry, we can get the basic parameters of the system or at least their relative values of components. To find out the basic information about system, we only need to know the light curve and its shape. From it, we can read parameters such as the period P, which is one of the most basic parameters. We can also find the duration of the brightness change D and also the "stopping" time at the brightness minimum d. After a learned approximation and modification of the equation 1.2 we can calculate the relative sizes of the components R_1, R_2

$$\frac{R_1}{r} = \frac{\pi}{2}\frac{D+d}{P}; \quad \frac{R_2}{r} = \frac{\pi}{2}\frac{D-d}{P}. \tag{1.6}$$

From the knowledge of the bolometric brightnesses at maxima B_0 and minima B_p/B_s,

we can also calculate the ratio of temperatures.

$$\frac{T_1^4}{T_2^4} = \frac{B_0 - B_p}{B_0 - B_s}.$$

(1.7)

From the ratio of the brightnesses at maximum and minimum in different parts of the spectrum, we can estimate the interstellar extinction values (Mikulášek and Zejda, 2013).

Adding other methods to photometry, such as spectroscopy, provides much more information and data about the studied systems. Spectroscopy gives us information about, for example, the radial velocities of components, their surface temperatures, or the composition of atmospheres. If we know the radial velocities V_1, V_2, we have a quick estimate of the mass ratio q, since

$$q = \frac{M_1}{M_2} = \frac{V_2}{V_1} = \frac{a_2}{a_1},$$

(1.8)

where a_1, a_2 are semi-major axes and M_1, M_2 are masses of components (Mikulášek and Krtička, 2005). For bounded system

$$a = a_2 + a_1.$$

(1.9)

Since we already know the period and semi-axis, we can calculate the sum of the masses ($M = M_1 + M_2$) from Kepler's third law

$$M = \frac{4\pi^2 a^3}{GP^2}.$$

(1.10)

Then we calculate the individual masses of the two components.
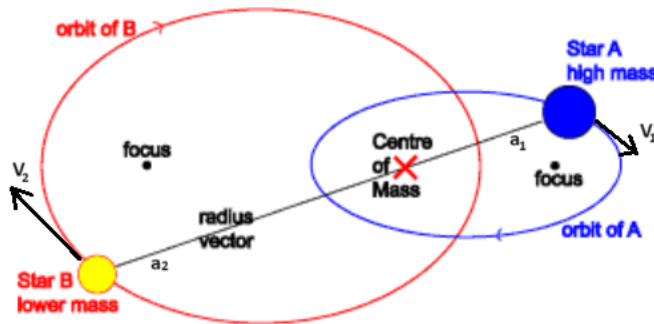
Figure 1.6: Illustration of orbits, Australian Telescope National Facility.

Furthermore, we can use the above-mentioned methods to obtain the distances of objects or to improve on already known parameters. Observing EBs allows us to study binary star systems and test theoretical models of stellar structure and evolution. The final stages of some systems are useful for studying extreme objects in the universe such as supernovae, neutron stars, black holes, etc. In addition, they can also serve for studying stellar populations, which allows analysis of the distribution of orbital periods across different groups of stars, the ratios of stellar masses within these binary systems. Very

useful for this are eccentric binaries with apsidal motion[1]. Unlike most binaries which have circular orbits, eccentric binaries move along elongated ellipses. For circular orbits, the secondary minimum in the phase diagram is exactly at 0.5. But in some cases, the secondary minimum can be displaced, which indicates, at first sight, the presence of eccentricity in the orbits of the components.

Likely, all systems will eventually reach circular trajectories. It can be a very long process called circularisation. This process and its duration are related to the relative sizes[2] (R/a) of the components in the system. So close stars should reach the circular orbits very quickly but the long-period ones still show signs of eccentricity. It is important to study the period-eccentricity relationship because there is expected to be a limit to the maximum value of eccentricity for a particular period (Zasche et al., 2021).

---

[1]Apsidial motion is the precession (rotation) of the line connecting the closest and the farthest point of objects with respect to each other.

[2]R = star radius, a = semi-major axis.

Chapter 2

Obtaining data

2.1 Photometry

As already mentioned, photometry is one of the basic observation methods. It is based on measuring the luminous flux. It is the amount of photons that come to us every second. Basically, it's a kind of quantification of the brightness. However, magnitudes are more commonly used for quantification. The relationship between magnitudes and the intensity of the signal coming to us is related in Pogson's equation where two stars are compared

$$m_1 - m_2 = -2.5 \log \frac{I_1}{I_2},$$
(2.1)

where m_1, m_2 are magnitudes of the stars and I_1, I_2 are intensities of their brightness. The brain also does logarithmic signal processing, which is why we use magnitudes in logarithmic scale. Some kind of comparison of the stars was started by Hipparchos in ancient Greece. By such observation, he compiled the first catalog of stars and divided them according to their brightness. The catalog contained approximately 850 stars (Hoffmann, 2017). Today, we know millions of confirmed variable stars, thanks to photometry (Watson and AAVSO).

In addition to visual photometry, in the past photographic or photoelectric photometry was also used. Today is the most used CCD or CMOS photometry. Even with these modern methods, the comparison is still used. We have to be sure that the comparison star is indeed non-variable, otherwise, it would skew the results. When measurements are taken, compared stars should have similar magnitudes and the same colors. There are two more stars marked for controlling cases. The stars are taken from the same star field as seen in the figure 2.1. The image is from an observation of HY CVn.

2.1.1 CCD photometry

As is already clear from the name of the method, we use CCD (charged-coupled device) sensors to capture the signal. The sensors are based on silicon technology that captures electromagnetic radiation (photons) coming from the source. The radiation produces electrons in the device and these accumulate in potential pits known as pixels. Pixels are mostly arranged in matrices. The number of electrons is directly proportional to the
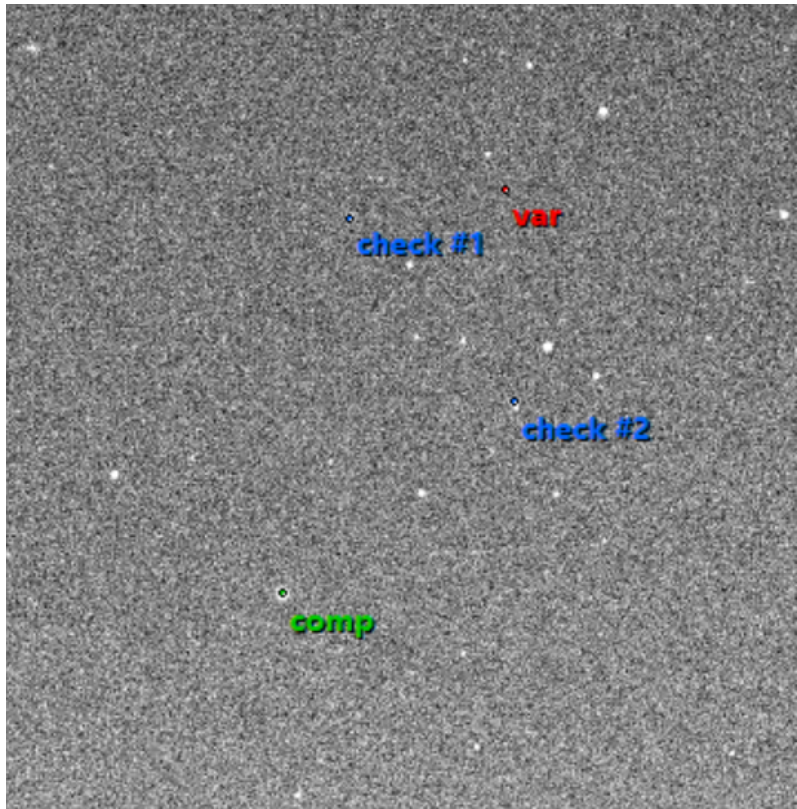
Figure 2.1: Picture of star field with the selected variable, comparison, and two control stars.

number of incoming photons. This linear characteristic is an advantage over other devices. It allows essentially arbitrary variation of exposure times. After a very long exposure, *blooming* occurs which is the overflow of electrons from the pixel. This can affect adjacent pixels. It often happens for extremely bright objects (see figure 2.4).
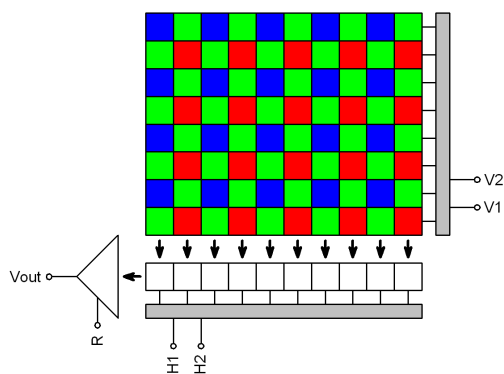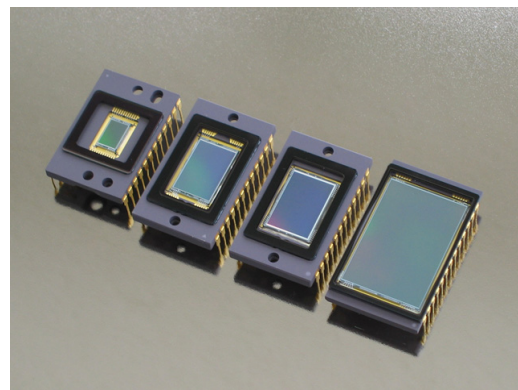

Figure 2.2: Scheme of RGB CCD (Moravian Instruments).

Figure 2.3: Diffrent types of CCDs (Moravian Instruments).
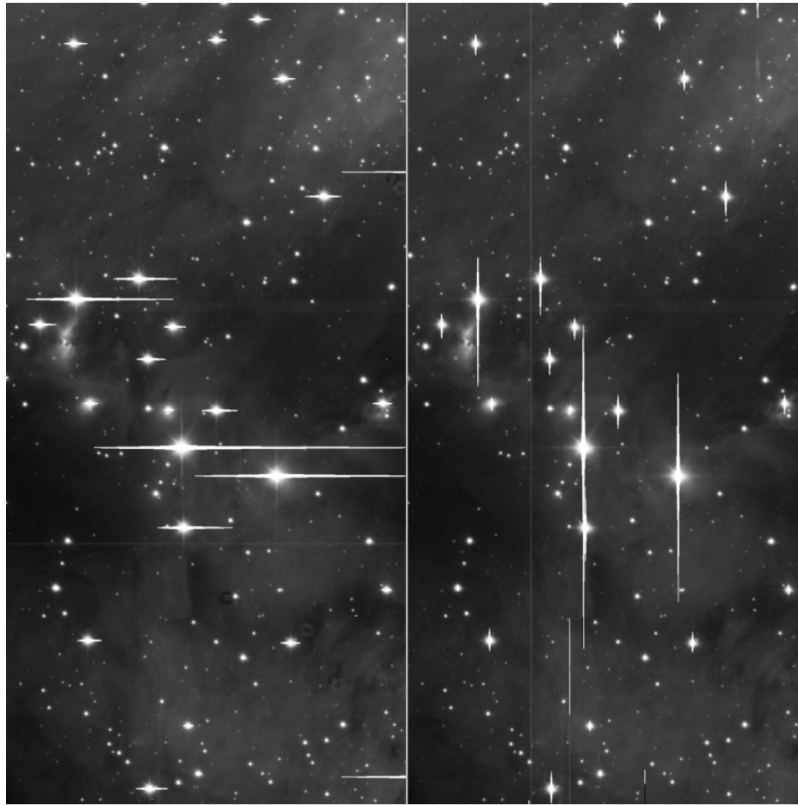
Figure 2.4: Blooming, (Pixlnsight).

CCD also has several undesirable properties. One of them is the dark current, which is produced by the thermal emission of electrons. Therefore, the sensor must be cooled. This is usually done with a Peltier device. All these parts are included in the CCD camera, connected to the telescope. Despite the cooling, the thermal current always appears in the final images. The so-called *dark frame* is used to remove it. This is taken with the camera covered so that no light hits the sensor. All that remains in such image is the noise of the dark current, which is then subtracted from the observed frames. The exposure of the dark frame is usually the same as the observation and the sensor is cooled at the same temperature. Several photos are taken, from which the median is then calculated and used to remove unwanted noise. The presence of *read out noise* is also undesirable. It is caused by the digitalization of the signal. It appears only once and always with the same intensity, so it is not difficult to remove it. Another correction that needs to be made are *flat fields*. Pixels have different sensitivities from the factory and the differences between single pixels can be up to 10 % (Janík, 2021). There may also be impurities on the apparatus that cannot be removed and we have to consider them. A flat field is taken against an evenly lighted background. Ideal for this purpose are images of the sky just before sunset or after sunrise. Then the stars are not visible and at the same time, the light from the sun does not disturb. Another option is to take the picture on an evenly lit smoothed surface in the dome interior. Flat fields are made separately for each filter in which we observe.

2.1.2 Photometric systems

All detectors can only record a certain part of the electromagnetic spectrum. This means that the maximum sensitivity may also be different. Internationally accepted filters have been developed to avoid misunderstandings in observations based on the use of different observing methods or different detectors. Many observations in the past have been recorded by the naked eye only. Therefore, it is likely that most of these measurements are around the yellow part of the spectrum. This is where our eyes have the best sensitivity. With the new methods, the differences between them were immediately visible. As each detector has a sensitivity to different wavelengths. For easier comparisons between methods, observational filters were invented.

The first photometric system was revealed to the world by Johnson and Morgan (1953). It was a broadband filter system called *UBV*. The range of each filter was defined also with its maximum throughput. Filter *U* has a maximum at 360 nm, *B* at 420 nm and *V* at 535 nm. In general, this system is still in use today. Later were added also *I*, *R*, *J*, *H*, *K* (AAVSO, 2022).

In addition to broadband systems, there are also midband and narrowband systems. While the broadband ones have a range of more than 30 nm, the narrowband ones have a range of less than 10 nm. These are mainly used to observe Hα spectral lines. The most well-known midband systems include the Strömgren's *uvby*. In addition to those already mentioned, there are many other systems. Some of them are compared in the figure 2.5.

2.2 Photometric surveys

Astronomical surveys play a crucial role in gathering data across extensive regions of the sky or numerous celestial objects. These comprehensive studies provide valuable insights into the universe's overall structure, identify new objects, and facilitate statistical analysis of celestial populations. Photometric surveys meticulously chart the brightness of the universe, while spectroscopic surveys delve into the properties of objects by analyzing their light. All-sky surveys, such as the SDSS, capture images of a significant portion of the sky, while targeted surveys concentrate on specific regions or types of objects (Abdurro'uf et al., 2022).

2.2.1 TESS

Transiting Exoplanet Survey Satellite (TESS) is a space telescope launched in 2018. The original duration of the project was supposed to be 2 years, but it has already been almost 6 years in operation and is still in progress. The main goal was to observe exoplanet transits, but it works very well for observing EBs. The detector uses the method of photometry with silicon CCD technology. It operates at wavelengths between 600 and 1000 nm which corresponds to the *I* and *R* filters combined (Ricker et al., 2015). This satellite observes continuously. It observes one part of the sky, which is called sector, for about 27 days and then moves on to the next. Some parts of the sky will be measured more often than others, depending on how TESS moves and maps the sky. To date (6.5.2024) this mission has confirmed 440 transiting objects and a further 7147 candidates (NASA).
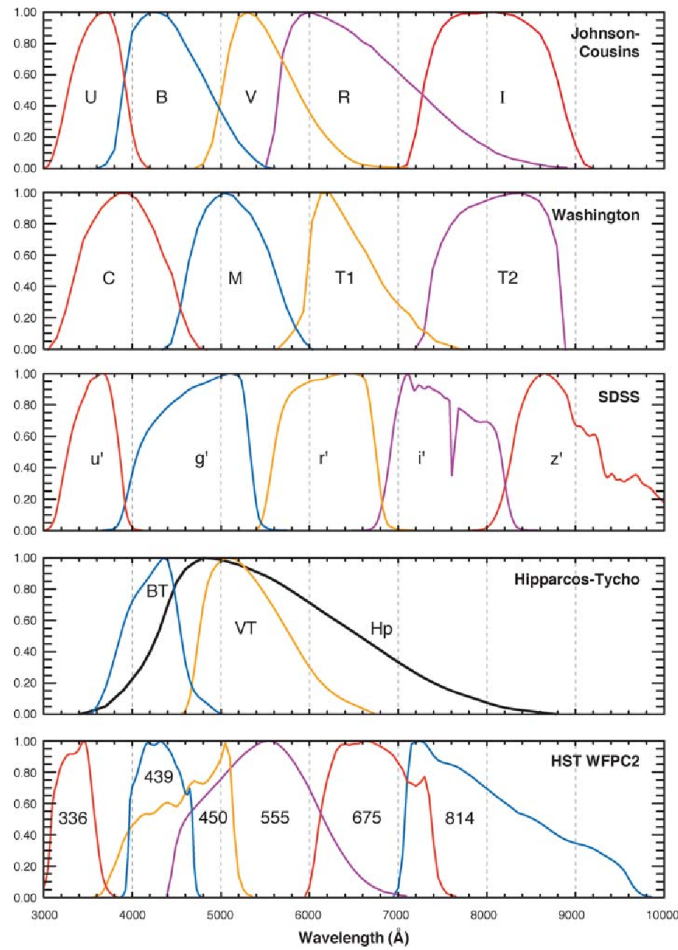
Figure 2.5: Exaples of photometric systems (Bessell, 2005).

We used a Python script written by Pejcha (2020). The script uses the *lightkurve* (Lightkurve Collaboration et al., 2018) library to download data from the TESS satellite survey. From the library, we use a function named *search_tesscut*. This function allows us to search for an object from the survey using its coordinates. We can then plot a map of the star field around the object we are looking for. At the same time we need to plot a 'mask' (see picture 2.6). This determines which object the function should focus on. Everything else around the mask is subtracted from the image. Then it is repeated for the comparison star. We get a graph of the flux with respect to time. The process have to be done for all available sectors. Using Pogson's equation, we calculate the brightness change for the star under study. The full script can be found in the appendix 4.1.

2.2.2   ASAS-SN

All Sky Automated Survey for SuperNovae (ASAS-SN) is a project focused on searching transiting objects in space. The project started in 2013 with two 14-cm telescopes, with further additions by 2020. Today it contains 24 different telescopes (and more will be added) situated all over the Earth. This allows you to continuously observe the entire
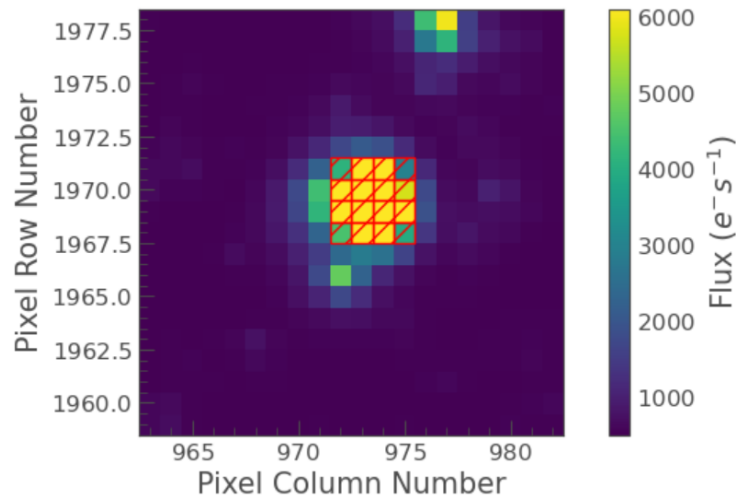
Figure 2.6: Star field and mask visualization.

visible sky. It is led by Ohio State University researchers. However, the observation itself needs no operator because it is fully automated. The project focuses on all visible variable objects brighter than 18 mag. Observations produce a huge amount of data. These are processed by a special program that recognizes the objects in the image and compares them with previous images. Next, it processes only those that indicate a change in brightness. The photometric data are publicly available as *Sky patrol* (ASAS-SN). From here the data were also used in this work, in *V* and *g* filters.

Chapter 3

Processing data

3.1 $O - C$ diagrams

One of the most important parameters in the observation of variable stars is the period of the brightness changes. Finding out the exact period value is sometimes a demanding task. Even if we know it, it may be that it has been determined incorrectly or even that the period may be changing over time. Astrophysicists use the $O - C$ diagram to detect these inaccuracies or changes. The principle is based on the assumption that changes always occur after exactly the same time interval. However, this is only true if the system is perfectly periodic.

So if we set some fundamental moment M_0 (most often this is given for a significant moment, e.g. the minimum of brightness), then the same minimum will occur exactly $M_0 + P$ later. In this way, we can make predictions over time. Since we know that our next chosen moment C occurs in exactly n periods, so

$$C = M_0 + nP, \tag{3.1}$$

where n is the whole number (Sterken, 2005). Equation 3.1 is generally valid, but in practice, time is usually calculated using E, which is specific to an object, according to equation 1.4. So, for example, if we want to find the time when the minimum of an EB occurs, we use:

$$C = M_0 + PE, \tag{3.2}$$

In multiple stellar systems, various phenomena that are not visible in short-term observation may occur. An $O - C$ diagram can be useful in detecting these phenomena as it provides a clear visual representation. The observed times (O) and the predictions (C) may not correspond as a result of some phenomenon. On the y-axis of the diagram we plot the difference between O and C, and on the x-axis we plot time t or epoch E. Several patterns can be seen in the graph, meaning a different phenomenon in the system. These patterns can be fitted with functions to determine the type of phenomenon.:

- Linear function:

  - Constant function with value 0. P and M_0 are determined correctly (see figure 3.1).

      – Constant shifted in the y-axis. *P* is correct, but M_0 have to be adjusted.

      – Non-zero straight line directive. *P* was determined incorrectly.

- Leap period change (see figure 3.3).

- Parabola: *P* is shortened or lengthened (see figure 3.2).

- Sinusoid: There is another body in the system (LiTE effect)(see figure 3.4).

- Sinusoid but primary and secondary minima have opposite phases: Apsidial motion (see figure 3.8).

- Complicated function: Multiple effects combined (see figure 3.8).

There may be other influences or a combination of those already mentioned entering the diagram. In this thesis, however, we will focus on eccentricity recognition from $O - C$ diagrams. Eccentricity will be indicated by the displacement of the primary and secondary minima apart in the y-axis. This means that secondary minima occur periodically but have a phase other than 0.5. [1]
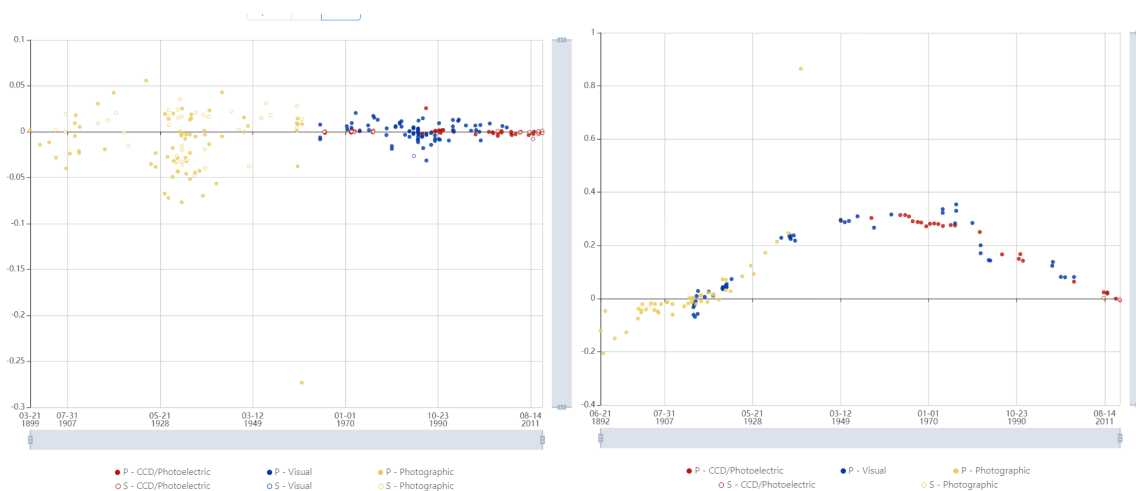
Figure 3.1: VZ CVn.

Figure 3.2: RS CVn: Period shortening.

---

[1]Figures used in chapter 3.1 are from: http://phoenix2.physics.muni.cz:8081/oc
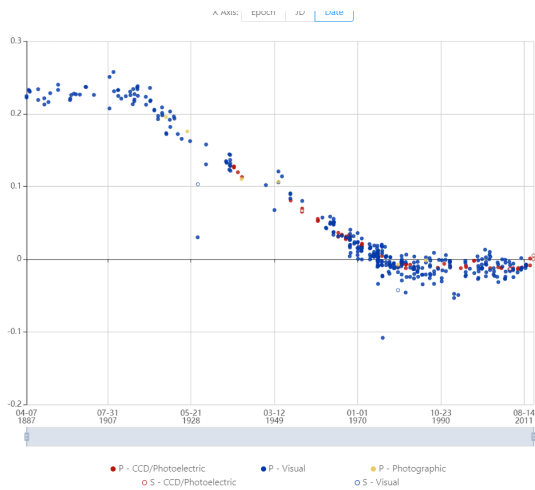
Figure 3.3: R CMa: Leap period change.
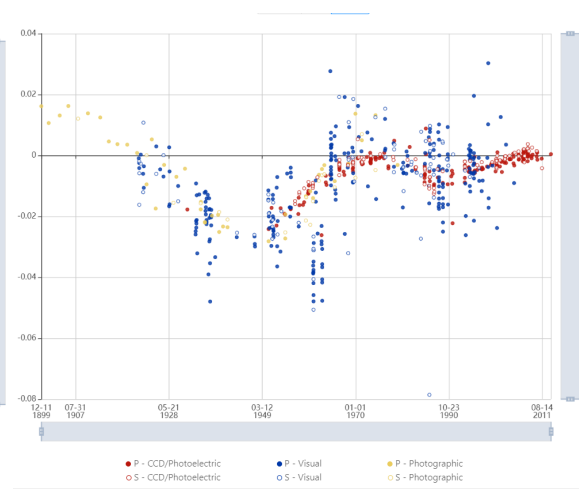
Figure 3.4: AK Her: LiTE effect.
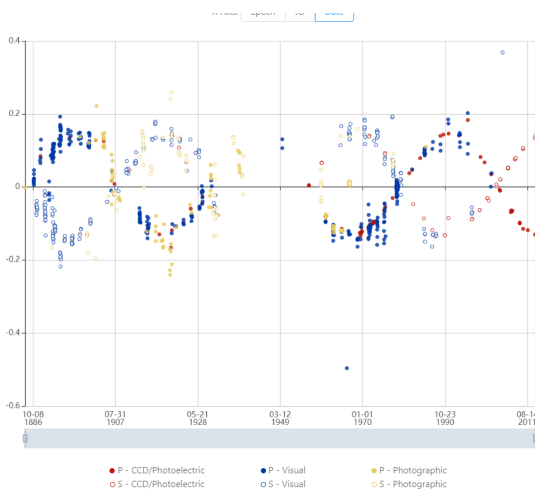
Figure 3.5: Y Cyg: Apsidial motion.
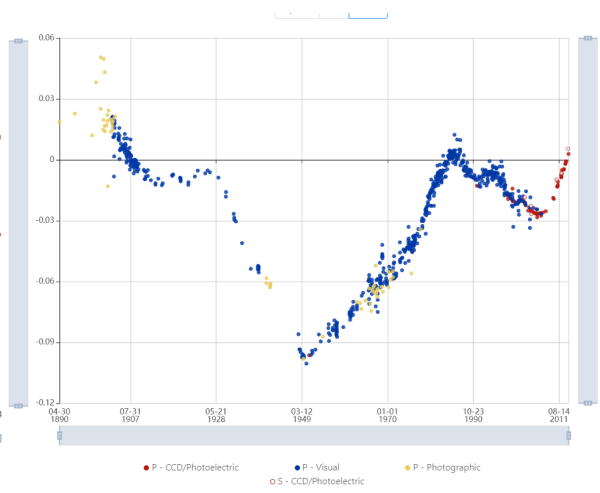
Figure 3.6: Z Dra: Combined effects.

3.2 Used programs

3.2.1 SILICUPS

Simple Light Curve Processing System (SILICUPS) is a light curve processing program especially for variable stars or exoplanets offered by Moravian Instruments (2019). We will use it to process both TESS and ASAS-SN data. This software allows us to record data containing time and magnitude changes. It will plot the obtained light curve. It also allows the calculation and plotting of the phase curve. From the shape of the phase curve, we can recognize the eccentricity of the system, due to the displacement of the secondary minima.

For each TESS sector, we process the data separately. In most cases, it is necessary to modify the basic ephemeris for fitting. In particular, the fundamental time M_0 has to be adjusted for phase offset. Otherwise, the program would not be able to fit the curve and create the model because it always takes the primary minimum at phase 0. The fitting in the case of the studied systems was relatively straightforward since they were Algol-type binaries.
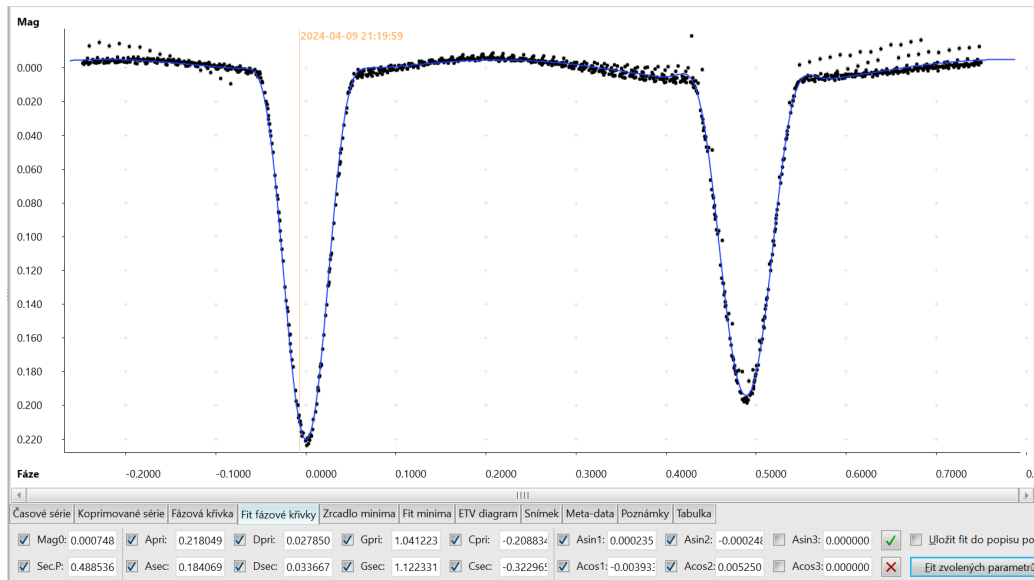
Figure 3.7: Fitting light curve in SILICUPS.

All data should be detrended. To do this, we use a function in the program that allows us to identify the residuals. Using the residuals, we can check how well our model fits the phase curve and then fit residuals using Python programming language. Chebyshev polynomials are best suited for the detrending process. There is a specific Python function for this from the numpy library (numpy.polynomial.Chebyshev.fit).[2] After detrending, it is now possible to fit a phase curve and determine all the minima timings. The program also plots $O - C$ diagrams but it is not enabled to analyze them. Therefore, we will use another program, which is described in the next chapter.

The processing of the ASAS-SN survey data had to be handled in a different way from that of the TESS satellite. There were often very few observations from these ground-based measurements, even over a longer duration of time. For this reason, it is not possible to determine the minima timings from the time series. We therefore divide the data into several parts according to the seasons when the observations were made. We plot a phase curve from one season in the program. From the difference between defined fundamental time M_0 and M_0 from the model of the light curve, that fit on current data, we get directly one point to $O - C$ diagram. So for each star, we get at least a couple of points. Since we need also an x-coordinate to plot but in most cases, there were no points exactly at the point of minimum, they had to be calculated using phase shift and period. With one available point around the minimum, we got an artificial point of minimum timing because it is just

_____

[2]For these purposes, my consultant Jakub Kolář provided me with a Python script that he created himself.
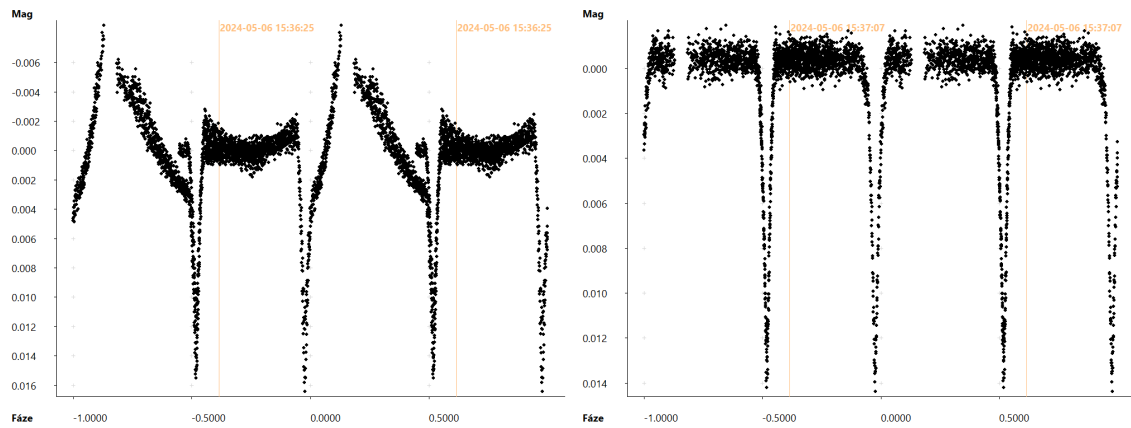
Figure 3.8: Phase curve of V1344 Her before (left) and after (right) detrending.

shifted by the phase multiplied by the period. For more accurate and easier processing, we used the phase curve model previously obtained from the TESS data.

3.2.2 OCFit

By processing the light curves, we obtained the minima timings. This information will be used for further calculation of $O - C$ and the subsequent creation of the graph (see chapter 3.1). For this purpose, we will use the OCFit software (Gajdoš and Parimucha, 2019). The program allows both calculation and graphical display.

First, a file containing the observed minima times needs to be uploaded. The program also needs the essential ephemerides: period P and the fundamental time M_0. The times C are calculated from the entered ephemerides, which then allows the plot of the $O - C$ diagram. In the case of eccentricity, it is also possible to adjust the phase dE when the secondary minima occurs or the software will estimate this value itself.

The data may contain some pattern caused by the phenomenon mentioned in the chapter 3.1. There are processing functions in the program for these cases. Fitting is possible by three different methods: Linear regression, Robust regression, or Monte Carlo. After the calculation, the data can be fitted with a linear function or a parabola. A linear function is usually used when the period is inaccurately determined but it remains constant over time. In cases where the period of the system changes, we use quadratic functions. After fitting data with the mentioned functions, it is possible to adjust the ephemerides if they were inaccurate. In our case, we will not adjust the parameter dE to see the eccentricity explicitly.
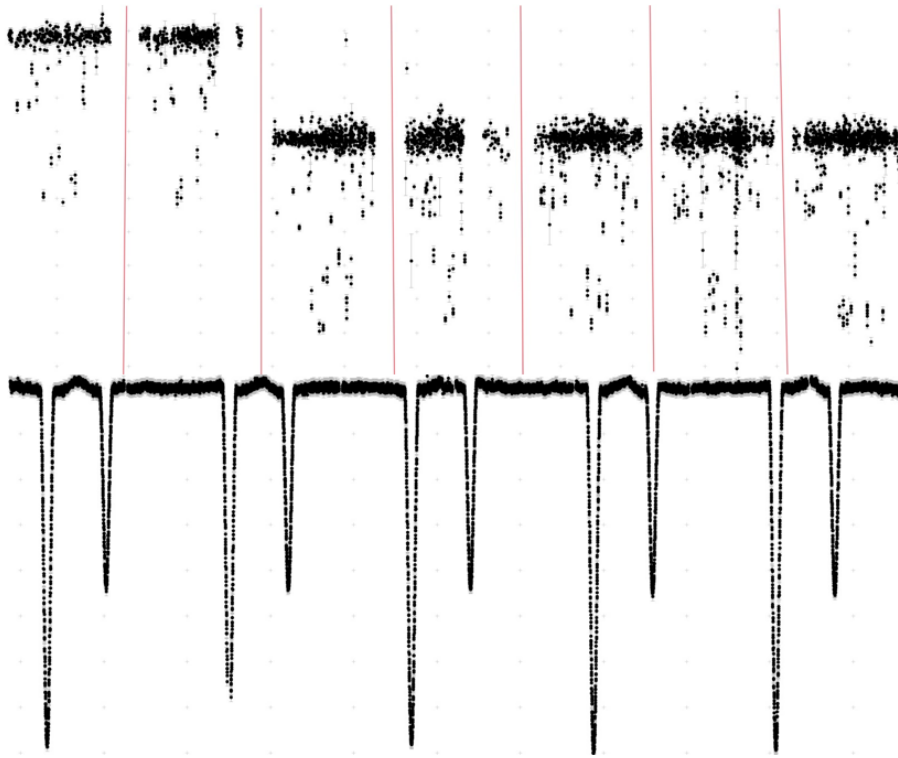
Figure 3.9: Comparison of time series from TESS (bottom) and ASAS-SN (top) and illustration of the splitting of the data into seasons (2MASS J10024347-5643283).
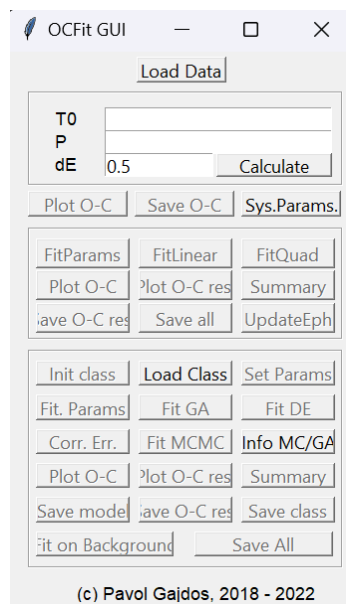
Figure 3.10: Main screen of OCFit.

Chapter 4

Selected objects

The title of this thesis indicates the main requirement taken into account in the selection of the studied objects. All of them should have been eclipsing binary stars with eccentric orbits, or at least candidates for such a classification. The stars were selected from the publication Kim et al. (2018) that examined 623 of these types of objects. It has been taken into account that the selected systems are less studied with no actual publications, which is also reflected in the fact that some objects do not yet have a definitive designation. All the studied objects are listed in table 4.1.

The main sources of used data were the TESS satellite and the ASAS-SN project surveys and thanks to the parameters of their equipment, we were not limited by the brightness when choosing stars. The properties of the surveys allowed us to select objects also with longer periods thanks to the consistent coverage of the night sky by the ASAS-SN survey and the cadence of the TESS observations. A slight disadvantage is the short duration of these projects as they have only been running for a few years so far.

In addition to the primary data source, two auxiliary databases were searched to supplement the analysis: the Czech *Phoenix*2 database[1] and the German *BAV* database. However, a major limitation of these databases is that both *Phoenix*2 and *BAV* contain mainly better-studied stars. Furthermore, the *BAV* database focuses only on the objects located in the northern hemisphere. As a result of these limitations, only five of the stars from each database were successfully selected. Three from *Phoenix*2 and two were contained in both databases.

Our initial intention was to gather additional data in Brno or Ždánice observatories to complement the existing dataset, we were unable to allocate the necessary time and expertise to conduct these observations effectively. The available observed data, after close examination, were not usable for our purposes. In addition to the Czech Republic, we had an opportunity of observing time at the La Silla Observatory in Chile, but we were unable to collect our own data because the predictions for none of our objects were favorable for our purposes. However, we asked for the help of Martin Mašek who agreed and, at our request, made two nights of observations for our one object at the Pierre Auger Observatory in Argentina on the FRAM telescope. Despite these setbacks, we are

---

[1]The database is taken from the older O-C gateway (http://var2.astro.cz/ocgate/?lang=cz), but with new design.

confident that the existing dataset provides a robust foundation for our research and will yield valuable insights into this thesis.

4.1   The results

The main task for the selected objects was to confirm or possibly disprove the eccentric orbits. It was also a matter of finding phenomena in the $O-C$ diagram that could confirm period shortening or lengthening, apsidal motion, or the presence of another body.

Firstly, we could comment on the eccentricity of the orbits, which has been confirmed for all the objects. This can be clearly seen in the figures in this chapter, which show $O-C$ diagrams of the studied stars. The vertical difference between the primary and secondary minima is seen in each diagram, which is an effect of the eccentricity. For comparison, figure 3.1 shows a diagram of an object with circular orbits. These statements are confirmed by the phase values in the table 4.1, which would only contain the value 0.5 for circular orbits because the secondary minima would occur exactly half a period after the primary minima. The phase values listed in the table, originate from a combined analysis of data acquired by the TESS and ASAS-SN surveys. Due to inconsistencies between the phase measurements obtained from TESS sectors and those from the single ASAS-SN seasons, the resultant phase values tabulated represent an average of the underlying measurements.

For the evaluation of the results from the $O-C$ diagrams[2], we will mainly focus on the data from the TESS satellite, which are all observed by a single equipment and subsequently processed by a single method. The measurements from the ASAS-SN survey are observed by different telescopes and, in addition, automatically processed by the system into the form in which we reached them. Despite the post-processing by us, there may be inconsistencies in the data compared to those from TESS. For the other data obtained, we have no information about the processing and therefore they are shown in the graphs mainly as visual complements to the dataset. For the reasons above, we separated the TESS data by color when necessary.

As already mentioned, all stars show signs of eccentricity. In most cases, no other interesting phenomenon is observed.

In the case of 2MASS J06430543-0034399 (fig. 4.21), it is not possible to make any conclusions about the system as we were unable to obtain almost any data apart from two measurements from the TESS satellite. The ASAS-SN survey contains a dataset for this object, but due to the data quality, it was not possible to determine the minima timings. This may be due to a combination of the system's long period and the measurements' low cadence.

We can also mention three objects that, at first view, have obviously very inconsistent data, namely: V339 Lac (figure 4.15), CF Mon (figure 4.17), FW Vul (4.20). In all cases, we have available older measurements, but these do not shed any light on the behavior of the system. Only a few of the points in the plot are from TESS or ASAS-SN, which also cover a short time interval. After all, we can conclude that the systems do not exhibit any interesting behavior that could be detected from the available data, and

---

[2]All points in the $O-C$ diagrams are obtained by CCD photometry, except for the few available photographic measurements, which are distinguished by a marker.

Name	RA [hms]	Dec [° ' "]	Period (d)	$M_0 - 2400000$	Phase	Mag (V)
2MASS J10024347-5643283	10 02 43.47	-56 43 28.29	10.940	52806.140	0,323	12.91
2MASS J04233735+2546360	04 23 37.34	+25 46 35.97	3.217	53735.215	0,461	13.10
V1107 Per	04 37 02.04	+42 05 51.95	1.455	54371.677	0,479	10.64
2MASS J06430543-0034399	06 43 05.43	-00 34 40.03	28.918	51618.030	0,238	12.99
2MASS J07303245-1611383	07 30 32.46	-16 11 38.40	2.686	54306.947	0,318	12.58
2MASS J07360305-5710149	07 36 03.05	-57 10 15.00	2.764	52390.219	0,457	11.51
2MASS J08453462-2158013	08 45 34.62	-21 58 01.34	11.042	54400.444	0,860	12.46
2MASS J11061317-3158400	11 06 13.17	-31 58 39.95	7.302	53187.419	0,274	12.49
DK CrB	16 11 17.95	+33 07 13.14	8.284	53505.806	0,518	13.83
V1344 Her	18 27 18.44	+19 08 33.30	7.146	54529.807	0,545	11.49
2MASS J20321743+5053479	20 32 17.43	+50 53 47.91	10.899	56375.475	0,410	12.72
V1110 Cas	01 30 05.44	+73 45 31.82	24.850	51478.455	0,706	10.33
V1162 Cas	02 08 31.90	+68 06 15.11	29.067	51427.643	0,230	10.72
V919 Cep	22 59 40.81	+65 12 40.11	1.852	51295.901	0,492	10.48
UW Cru	12 14 03.85	-64 40 55.14	6.354	25362.221	0,532	12.30
V339 Lac	22 11 59.25	+53 00 45.19	3.409	34006.066	0,509	12.90
AT Lep	05 48 17.06	-25 02 30.73	10.649	52634.787	0,449	11.56
CF Mon	06 49 21.99	-00 23 46.52	2.610	30047.640	0,512	13.20
V370 Sge	20 04 59.88	+20 13 28.31	8.326	52734.955	0,379	11.80
V2184 Sgr	19 46 17.49	-37 24 52.66	16.495	53214.525	0,231	12.70
FW Vul	19 40 51.25	+27 13 01.35	4.526	34706.111	0,495	12.23

Table 4.1: Studied objects. The 'Phase' column indicates at what phase of the period the secondary eclipse occurs.

more precise observations would be needed. The inconsistency of the earlier data may be due to observations in different filters, but the *Phoenix*2 does not contain data about used filters. This is one possible explanation although unlikely as ASAS-SN also contains multiple filters and there was no visible difference. In these three cases, we can also see the inaccuracy of the data observed by the older methods, which are marked with triangular markers.

The $O-C$ diagram constructed for the binary systems 2MASS J07360305-5710149 (figure 4.5) and 2MASS J04233735+2546360 (figure 4.2) reveals distinct linear trends for the primary and secondary components, with opposite slopes. This may indicate a sinusoidal pattern, which tends to be caused by the apsidal motion of the system. To reach any definitive conclusions, we would need more long-term observations to be able to confirm the described phenomenon. A similar change is also found in figure 4.13 for the V919 Cep. Here, analysis of the TESS data provided evidence consistent with apsidal motion. However, the remaining dataset, from other observations, exhibits inconsistencies that prevent a definitive confirmation. A certain profile is also visible in these data, but without more information about the observation and post-processing methods, we cannot be confident about the data accuracy.

To summarise, we can say that more observations are needed, especially from TESS or other similar satellites that can provide better and more accurate measurements than other sources. For further results, it would be necessary to make a model for each system (e.g. in the PHOEBE program) or to have access to spectroscopic data.
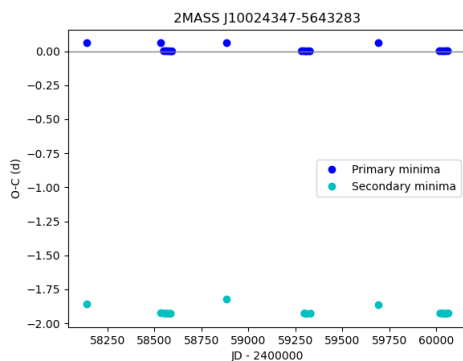
Figure 4.1: $O-C$ diagram of star 2MASS J10024347-5643283
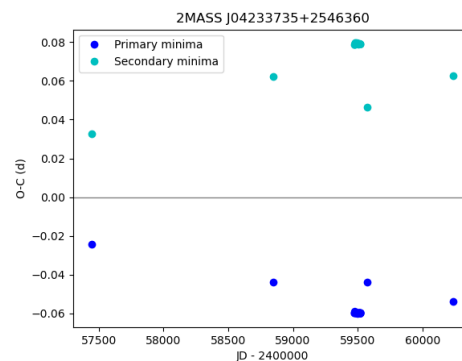
Figure 4.2: $O-C$ diagram of star 2MASS J04233735+2546360
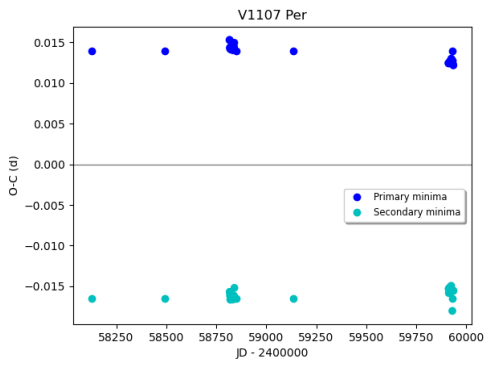
Figure 4.3: $O-C$ diagram of star V1107 Per
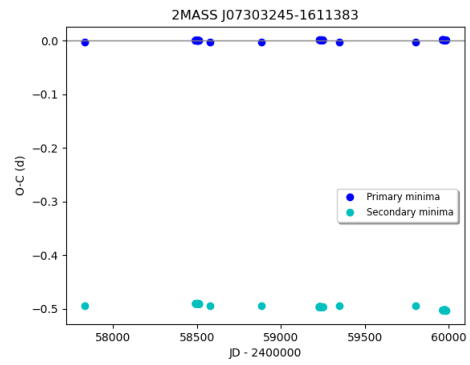
Figure 4.4: $O-C$ diagram of star 2MASS J07303245-1611383
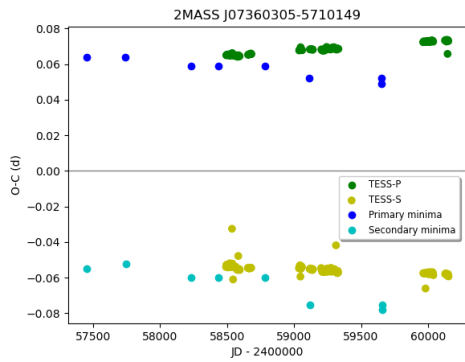
Figure 4.5: $O-C$ diagram of star 2MASS J07360305-5710149
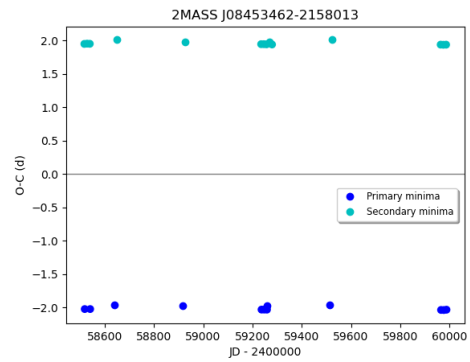
Figure 4.6: $O-C$ diagram of star 2MASS J08453462-2158013
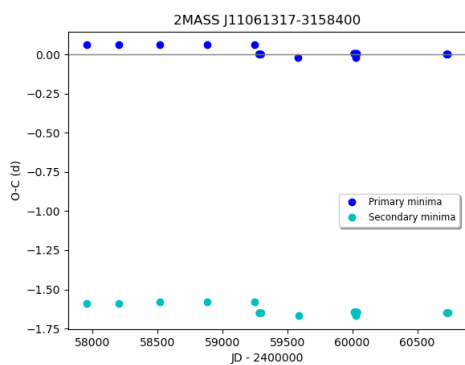
Figure 4.7: $O-C$ diagram of star 2MASS J11061317-3158400
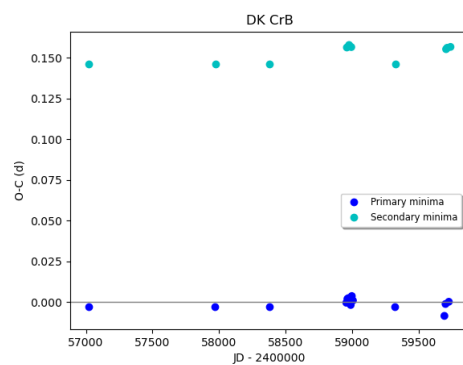
Figure 4.8: $O-C$ diagram of star DK CrB
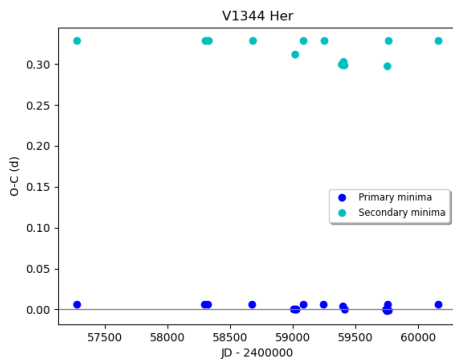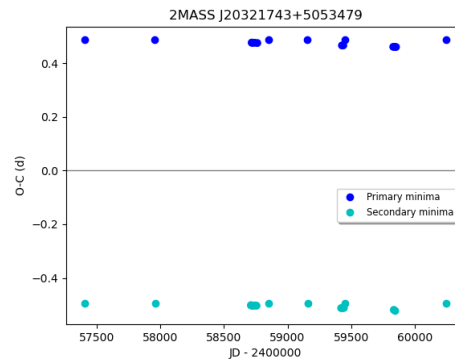
Figure 4.9: $O-C$ diagram of star V1344 Her

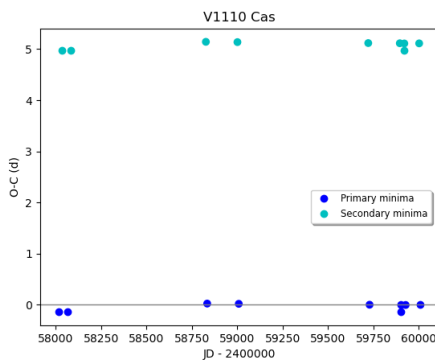
Figure 4.10: $O-C$ diagram of star 2MASS J20321743+5053479
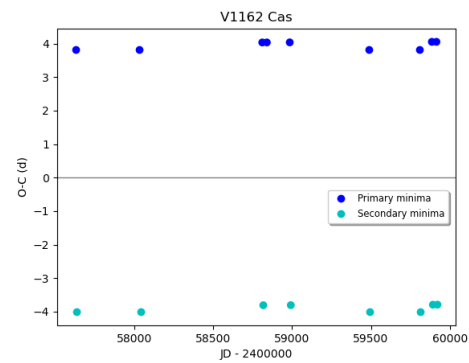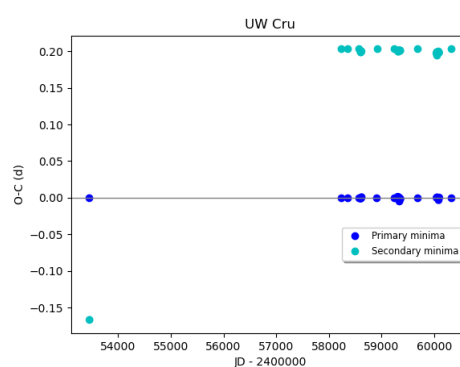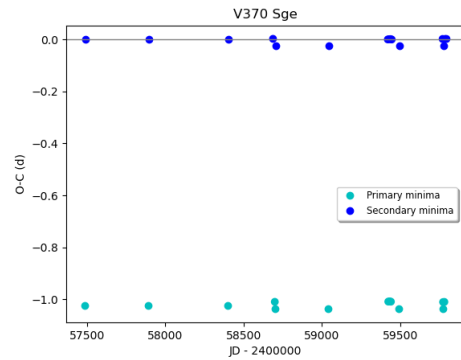

Figure 4.11: $O-C$ diagram of star V1110 Cas

Figure 4.12: $O-C$ diagram of star V1162 Cas
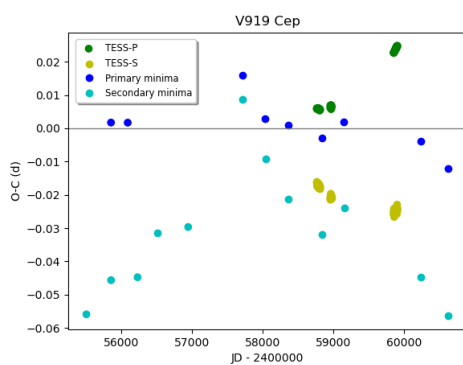
Figure 4.13: $O-C$ diagram of star V919 Cep

Figure 4.14: $O-C$ diagram of star UW Cru
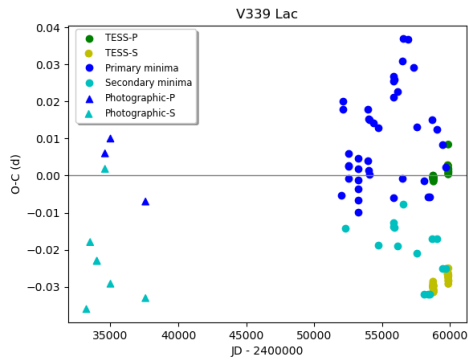
Figure 4.15: $O - C$ diagram of star V339 Lac
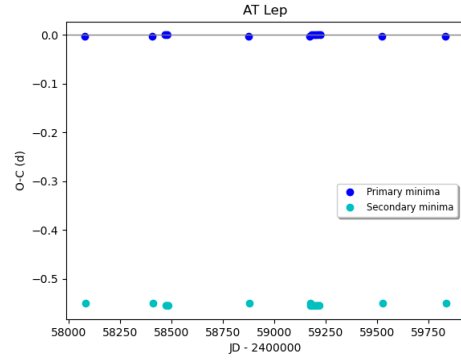
Figure 4.16: $O - C$ diagram of star AT Lep
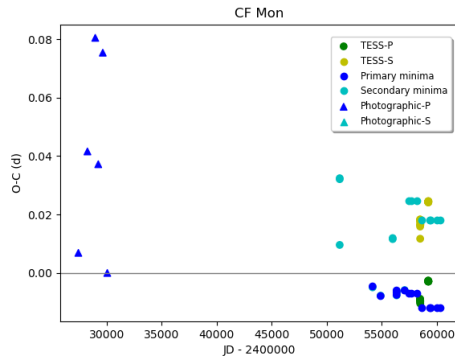
Figure 4.17: $O - C$ diagram of star CF Mon

Figure 4.18: $O - C$ diagram of star V370 Sge
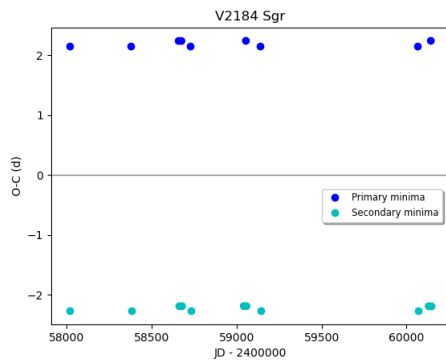
Figure 4.19: $O - C$ diagram of star V2184 Sgr
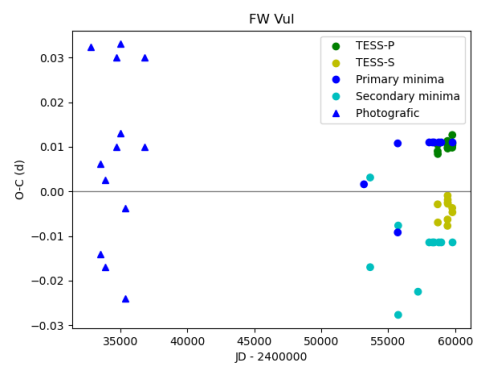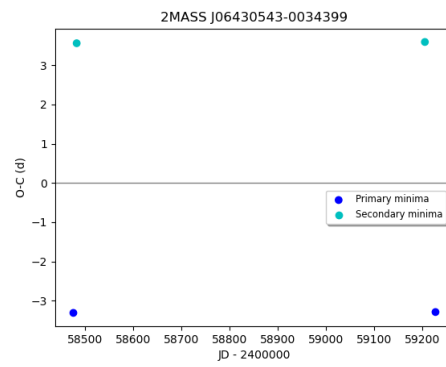

Figure 4.20: $O - C$ diagram of star FW Vul

Figure 4.21: $O - C$ diagram of star
2MASS J06430543-0034399

Conclusion

This bachelor thesis focused on the study of 21 eclipsing eccentric binaries, which have not been extensively researched or published to date. To achieve this goal, we processed photometric data from the TESS satellite and the ASAS-SN survey. ASAS-SN allows to download light curves directly but for TESS we had to use a Python script and the *lightkurve* function. From the obtained data we constructed phase curves in SILICUPS and determined the minima timings. The datasets from these two sources had to be processed by different methods due to the difference in the accuracy of the measurements.

Subsequently, we compared the observed minima timings with the values calculated based on existing ephemeris, which allowed us to construct $O-C$ diagrams. It was also necessary to use different methods to extract information into diagrams. The TESS data could be processed in OCFit, which calculates the values of $O-C$ from the available ephemeris and also allows to specify the ephemeris. We processed the ASAS-SN data using a method where we tried to fit a model to the phase curve as precisely as possible and then obtained the $O-C$ values by subtracting the M_0 of the model from the original M_0. We also supplemented the diagrams with available data from earlier publications. After analyzing these $O-C$ diagrams, we were able to confirm eccentricity for all objects, and we also found some possible phenomena that these systems could undergo, such as apsidal motion or period changes. In addition to diagrams, we summarized basic information about studied objects, such as their phases, magnitudes, and periods.

It should be noted, however, that we were limited in the analysis by the availability of observational data and the time frame of the bachelor's thesis. For further and comprehensive results of the studied objects, it would be necessary to continue research using longer time series and spectroscopic observations.

Thus, in this work, we have contributed to expanding our knowledge of poorly studied eclipsing eccentric binaries. The obtained results can be useful for further research of these objects and for testing stellar evolution models.

Despite these limitations, we believe that we have contributed to expanding our knowledge of studied eclipsing eccentric binaries. The obtained results open the way for further research of these interesting astrophysical objects and for testing stellar evolution models.
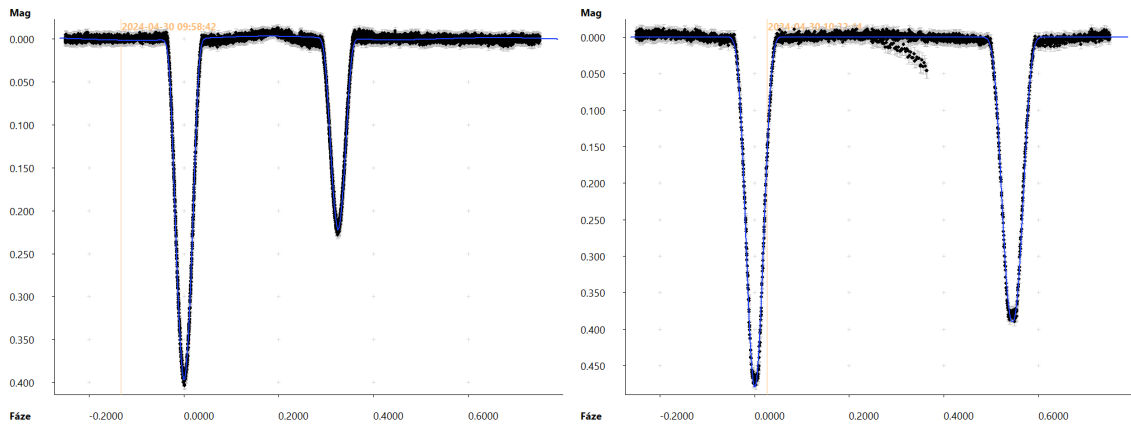
Appendix

Phase curves

Figure 4.22: 2MASS J10024347-5643283 (left), 2MASS J04233735+2546360 (right)
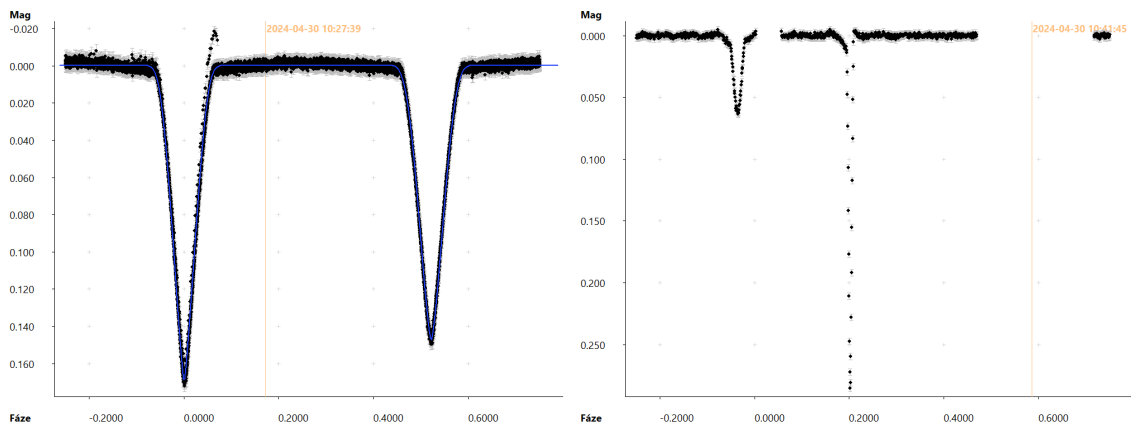

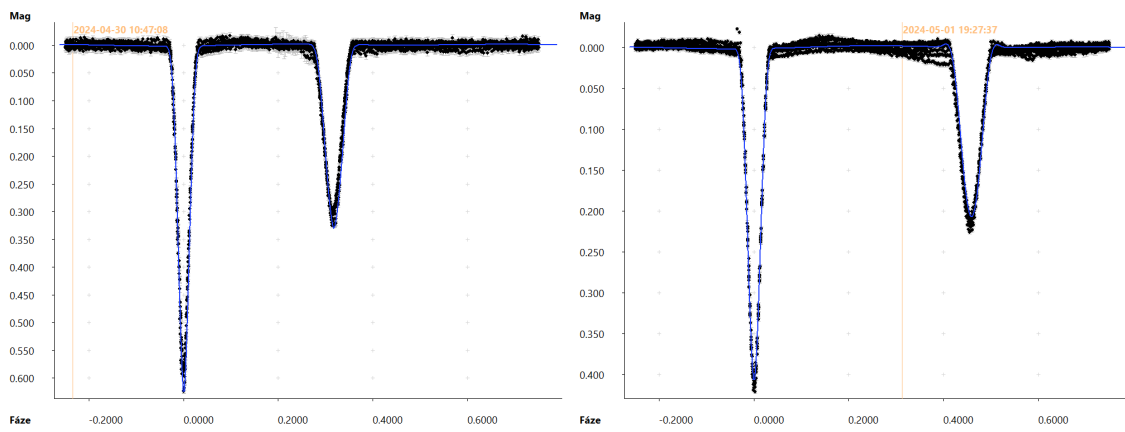Figure 4.23: V1107 Per (left), 2MASS J06430543-0034399 (right)

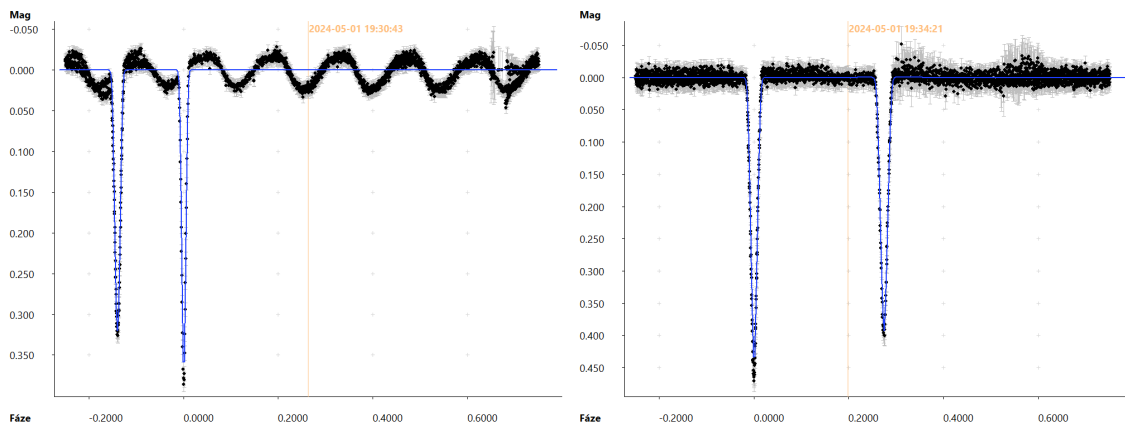Figure 4.24: 2MASS J07303245-1611383 (left), 2MASS J07360305-5710149 (right)

Figure 4.25: 2MASS J08453462-2158013 (left): The graph shows another phenomenon besides the occultations. It could be a pulsation with 1.579 days period., 2MASS J11061317-3158400 (right)
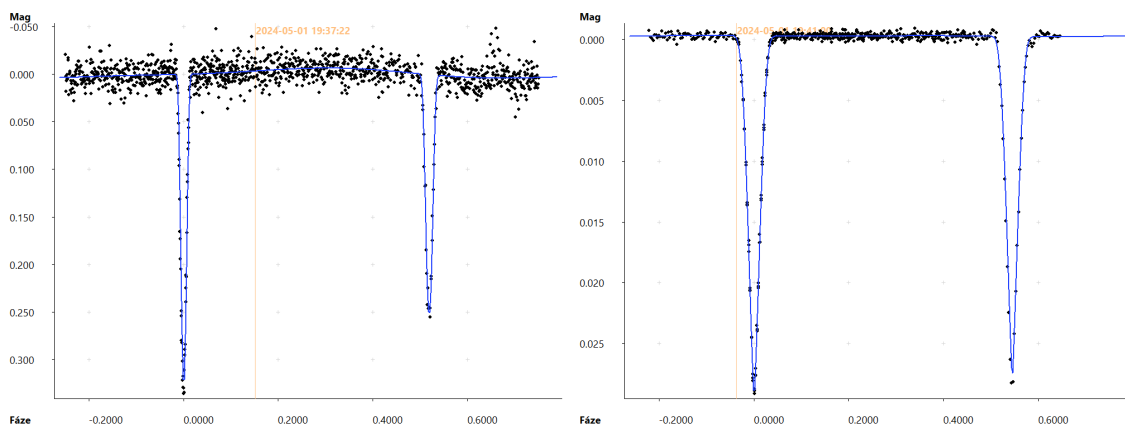

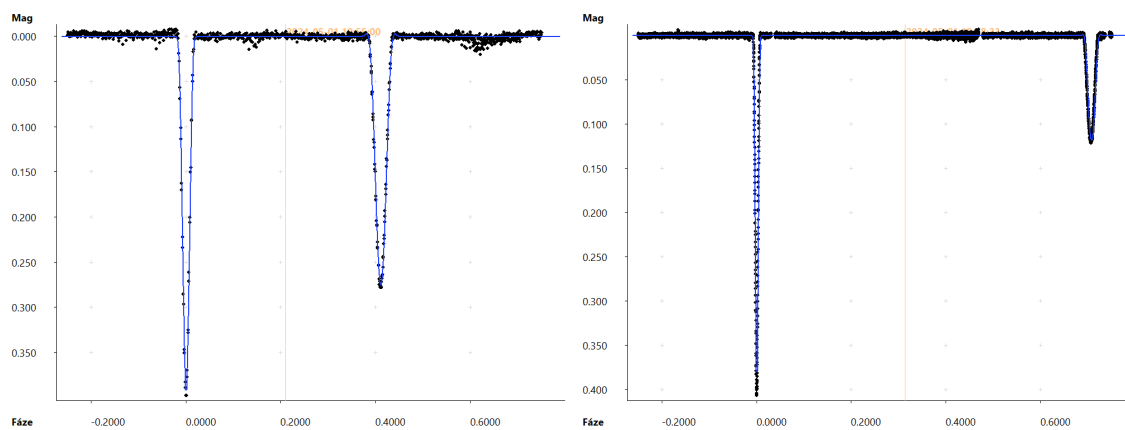Figure 4.26: DK CrB (left), V1344 Her (right)

Figure 4.27: 2MASS J20321743+5053479 (left), V1110 Cas (right)
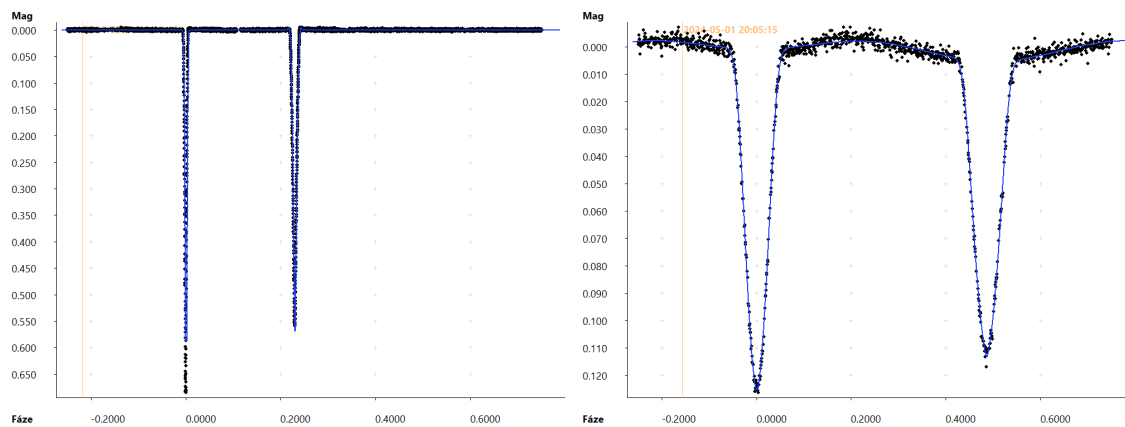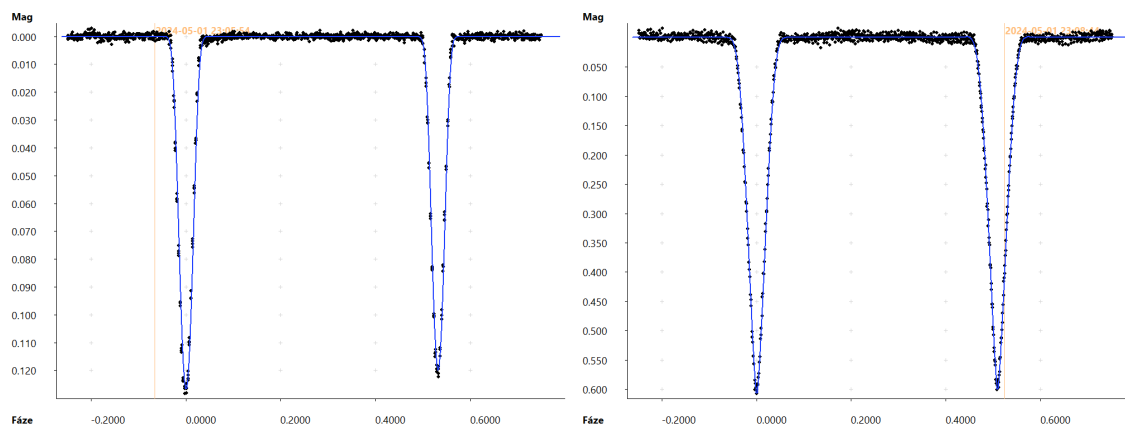

Figure 4.28: V1162 Cas (left), V919 Cep (right)

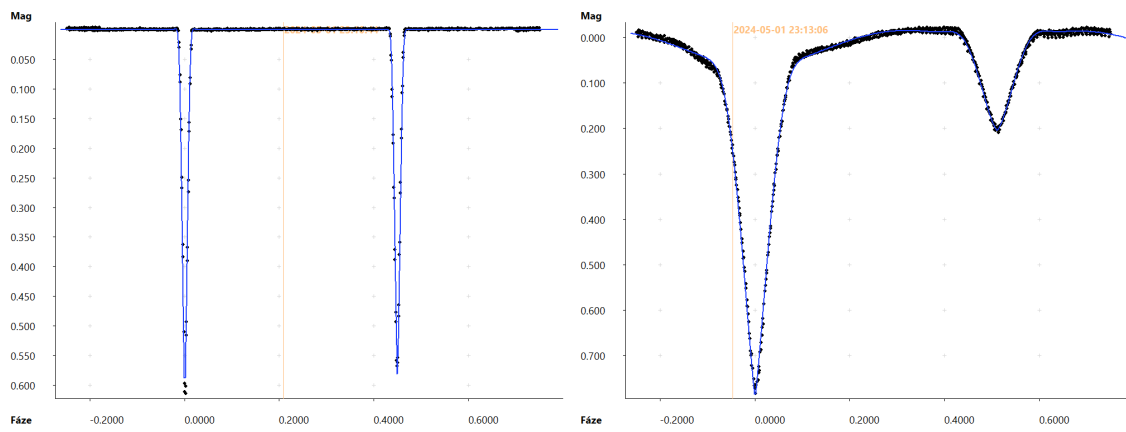Figure 4.29: UW Cru (left), V339 Lac (right)
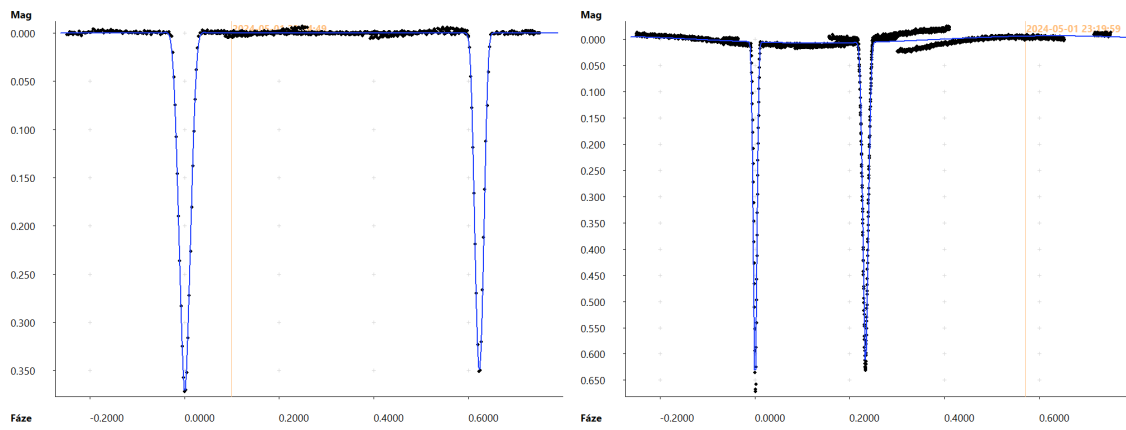
Figure 4.30: AT Lep (left), CF Mon (right)

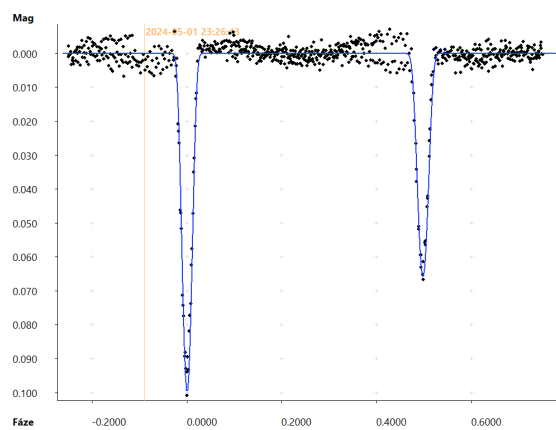Figure 4.31: V370 Sge (left), V2184 Sgr (right)

Figure 4.32: FW Vul

Python script

Listing 4.1: Python script for downloading TESS data.

```python
import pandas as pd
import numpy as np
import math
import lightkurve as lk
import matplotlib.pyplot as plt
get_ipython().run_line_magic('matplotlib', 'inline')

search_results = lk.search_tesscut("RA DE")
search_results

tpfs = search_results.download_all(cutout_size=20,quality_bitmask='
    hardest')

i =
tpfs[i].plot()

target_mask = tpfs[i].create_threshold_mask(threshold = 190,
    reference_pixel = 'center')
target_mask [9:12,9:12] = 1
tpfs[i].plot(aperture_mask = target_mask, mask_color = 'r')
n_target_pixels = target_mask.sum()
n_target_pixels

target_lc = tpfs[i].to_lightcurve(aperture_mask = target_mask)
bg_mask = ~tpfs[i].create_threshold_mask(threshold = 0.0001,
    reference_pixel = None)
tpfs[i].plot(aperture_mask = bg_mask, mask_color = 'w')

n_bg_pixels = bg_mask.sum()
n_bg_pixels

bg_lc_per_pixel = tpfs[i].to_lightcurve(aperture_mask = bg_mask)/
    n_bg_pixels
bg_estimate_lc = bg_lc_per_pixel * n_target_pixels
corr_lc = target_lc - bg_estimate_lc.flux
corr_lc.plot()

corr_lc.flatten(5001).plot()

corr_lc.time = corr_lc.time+tpfs[i].get_keyword('BJDREFI')+tpfs[i].
    get_keyword('BJDREFF')
name = "star{}".format(i)+".csv"
corr_lc.flatten(5001).to_csv(name)

perioda =
M0 =
corr_lc.flatten(5001).fold(perioda, t0 = M0).scatter()

search_results_cmp = lk.search_tesscut('RA DE')
search_results_cmp
```

```
tpfs_cmp =search_results_cmp.download_all(cutout_size=20,
    quality_bitmask='hardest')

i =
tpfs_cmp[i].plot()

target_mask_cmp = tpfs_cmp[i].create_threshold_mask(threshold = 150,
    reference_pixel = 'center')
target_mask_cmp[9:12,9:12] = 1

tpfs_cmp[i].plot(aperture_mask = target_mask_cmp, mask_color = 'r')
n_target_cmp_pixels = target_mask_cmp.sum()
n_target_cmp_pixels

target_cmp_lc = tpfs_cmp[i].to_lightcurve(aperture_mask =
    target_mask_cmp)
bg_mask_cmp = ~tpfs_cmp[i].create_threshold_mask(threshold = 0.001,
    reference_pixel = None)
n_bg_cmp_pixels = bg_mask_cmp.sum()

bg_cmp_lc_per_pixel = tpfs_cmp[i].to_lightcurve(aperture_mask =
    bg_mask_cmp)/n_bg_cmp_pixels
bg_estimate_cmp_lc = bg_cmp_lc_per_pixel * n_target_cmp_pixels
corr_cmp_lc = target_cmp_lc - bg_estimate_cmp_lc.flux

corr_cmp_lc.time = corr_cmp_lc.time+tpfs_cmp[i].get_keyword('BJDREFI
    ')+tpfs_cmp[1].get_keyword('BJDREFF')
name_cmp = "star_cmp_{}".format(i)+".csv"
corr_cmp_lc.flatten(5001).to_csv(name_cmp)

for i in range(len(tpfs)):
    name = "star{}".format(i)+".csv"
    name_cmp = "star_cmp_{}".format(i)+".csv"
    variable = pd.read_csv(name, thousands = r" ", sep = ",",
        decimal = ".")
    comparison = pd.read_csv(name_cmp, thousands = r" ", sep = ",",
        decimal = ".")
    change_data =pd.concat([variable["time"],comparison["time"],
        variable["flux"],comparison["flux"],variable["flux_err"],
        comparison["flux_err"]],axis =1)
    change_data.columns = ["var_time", "comp_time", "var_flux", "
        comp_flux", "var_flux_err", "comp_flux_err"]
    change = -2.5*np.log10(change_data["var_flux"]/change_data["
        comp_flux"])
    error = (((2.5*change_data["comp_flux_err"])/change_data["
        var_flux"])**2+((2.5*change_data["var_flux_err"])/change_data
        ["comp_flux"])**2)**0.5
    ch = change.tolist()
    final_change = []
    for j in range(len(ch)):
        a = ch[j]
        x = "%.17f" % a
        final_change.append(x)
    change = pd.Series(final_change)
```

```
err = error.tolist()
final_error = []
for k in range(len(err)):
    b = err[k]
    y = "%.17f" % b
    final_error.append(y)
error = pd.Series(final_error)
time = variable["time"]
final_data = pd.concat([time, change, error], axis = 1)
final_name = "star{}".format(i)+"_final.txt"
np.savetxt(final_name,final_data,fmt='%s',delimiter='\t' )
```

Bibliography

AAVSO. AASVO Guide to CCD/CMOS Photometry. *Cambridge*, 2022. ISBN 978-1-939538-62-8.

Abdurro'uf, K. Accetta, and C. Aerts. The Seventeenth Data Release of the Sloan Digital Sky Surveys: Complete Release of MaNGA, MaStar, and APOGEE-2 Data. *The Astrophysical Journal Supplement Series*, 259(2), Mar. 2022. doi: 10.3847/1538-4365/ac4414. URL https://dx.doi.org/10.3847/1538-4365/ac4414.

ASAS-SN. Sky patrol. https://asas-sn.osu.edu/?ra=102.34167dec=-0.39625; (Accessed: 2024-04-06).

Australian Telescope National Facility. Introduction to Binary Stars. URL https://www.atnf.csiro.au/outreach/education/senior/astrophysics/binary_intro.html. Accessed: 2024-03-26.

M. Bessell. Standard photometric systems. *Aug Annu. Rev. Astron. Astrophys*, 11:293–336, 09 2005. doi: 10.1146/annurev.astro.41.082801.100251.

M. Čokina, M.-K. V., and B. P. Automatic classification of eclipsing binary stars using deep learning methods. *Astronomy and Computing*, 2021. ISSN 2213-1337. doi: https://doi.org/10.1016/j.ascom.2021.100488. URL https://www.sciencedirect.com/science/article/pii/S2213133721000421.

P. Gajdoš and Š. Parimucha. New tool with GUI for fitting O-C diagrams. *Open European Journal on Variable Stars*, 197:71, Apr. 2019.

S. M. Hoffmann. Hipparchs Himmelsglobus: Ein Bindeglied in der babylonisch-griechischen Astrometrie? 2017. doi:10.1007/978-3-658-18683-8., ISBN 978-3-658-18683-8.

J. Janík. Astronomické pozorování. 2021. Masaryk university.

L. Jetsu, S. Porceddu, and e. a. Lyytinen. Did the ancient egyptians record the period of the eclipsing binary algol—the raging one? *The Astrophysical Journal*, 773(1):1, July 2013. ISSN 1538-4357. doi: 10.1088/0004-637x/773/1/1. URL http://dx.doi.org/10.1088/0004-637X/773/1/1.

H. Johnson and W. Morgan. Fundamental stellar photometry for standards of spectral type. *Astrophysical journal*, 1953.

C. H. Kim, J. M. Kreiner, and B. Zakrzewski. A Comprehensive Catalog of Galactic Eclipsing Binary Stars with Eccentric Orbits Based on Eclipse Timing Diagrams. , 235 (2):41, Apr. 2018. doi: 10.3847/1538-4365/aab7ef.

Lightkurve Collaboration, J. V. d. M. Cardoso, C. Hedges, M. Gully-Santiago, and et al. Lightkurve: Kepler and TESS time series analysis in Python. Astrophysics Source Code Library, record ascl:1812.013, Dec. 2018.

Z. Mikulášek and J. Krtička. Úvod do fyziky hvězd. *Masaryk University*, 2005.

Z. Mikulášek and M. Zejda. Úvod do studia proměnných hvězd. *Masaryk University*, 2013. ISBN 978-80-210-6241-2.

Moravian Instruments. Úvod do techniky CCD čipů. URL `https://www.gxccd.com/art?id=303&lang=405`. Accessed: 2024-03-26.

Moravian Instruments. SImple LIght CUrve Processing System. 2019. URL `https://www.gxccd.com/cat?id=187&lang=405`. Accessed: 2024-03-22.

NASA. Transiting exoplanet survey satellite (tess). URL `https://exoplanets.nasa.gov/tess/`.

O. Pejcha. Světelné křivky z TESS. *Sekce proměnných hvězd a exoplanet ČAS*, Nov. 2020. URL `https://www.youtube.com/watch?v=47g7ypzHTRI`. Provided by the SAO/NASA Astrophysics Data System.

J. R. Percy. Understanding Variable Stars. *Cambridge University Press*, 2007.

Pixlnsight. NGC 6914 with Calar Alto Observatory: Processing Notes. URL `https://pixinsight.com/examples/NGC6914-CAHA/index.html`. Accessed: 2024-03-26.

G. R. Ricker, J. N. Winn, and R. Vanderspek. Transiting Exoplanet Survey Satellite (TESS). *Journal of Astronomical Telescopes, Instruments, and Systems*, 1:014003, Jan. 2015. doi: 10.1117/1.JATIS.1.1.014003.

C. Sterken. The o-c diagram: Basic procedures. *The Light-Time Effect in Astrophysics, Proceedings of ASP Conference Series*, 335:3–11, 2005. doi: 2005ASPC..335....3S.

C. Sterken and C. Jaschek. Light Curves of Variable Stars, A Pictorial Atlas. 1996.

C. Watson and AAVSO. The international variable star index (vsx). https://www.aavso.org/vsx/index.php; (Accessed: 2024-05-03).

P. Zasche, Z. Henzl, and M. Mašek. Hunt for extremely eccentric eclipsing binaries. , 652: A81, Aug. 2021. doi: 10.1051/0004-6361/202141052.

M. Zeilik and S. Gregory. Introductory Astronomy and Astrophysics. 1998.